Dissertations
Department of Chemistry
University of Eastern Finland

No. 141 (2017)

Ville Nissinen

The roles of multidentate ether and amine electron donors in the crystal structure formation of magnesium chloride supports

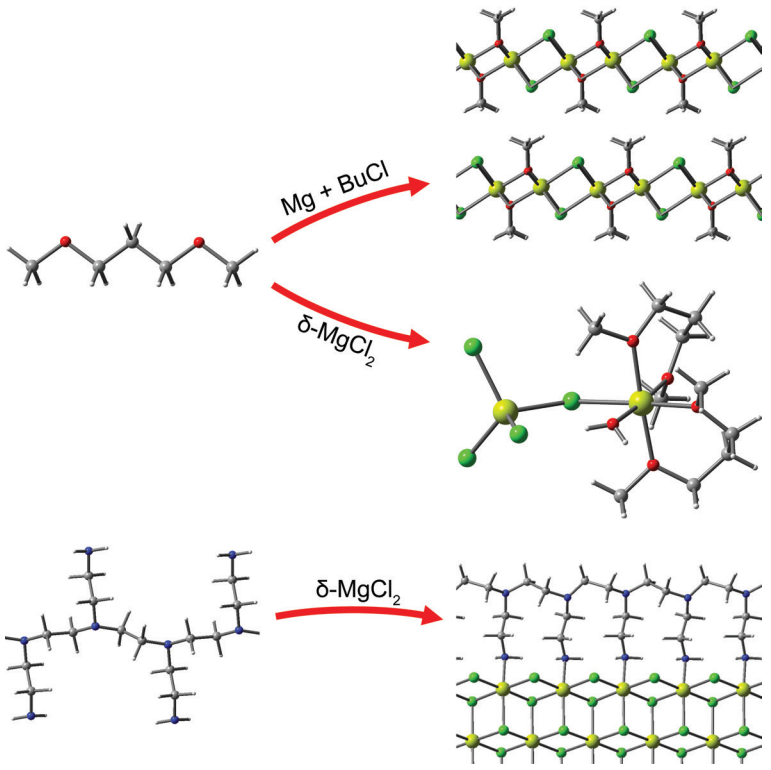

The roles of multidentate ether and amine electron donors in the crystal structure formation of magnesium chloride supports

Ville Nissinen

Department of Chemistry
University of Eastern Finland
Finland

Joensuu 2017

Ville Nissinen
Department of Chemistry, University of Eastern Finland
P.O. Box 111, FI-80101 Joensuu, Finland

Supervisor
Prof. Tuula Pakkanen, University of Eastern Finland, Joensuu, Finland

Referees
Prof. Matti Haukka, University of Jyväskylä, Jyväskylä, Finland
Prof. Timo Repo, University of Helsinki, Helsinki, Finland

Opponent
Prof. Reko Leino, Åbo Akademi University, Turku, Finland

To be presented with the permission of the Faculty of Science and Forestry of the University of Eastern Finland for public criticism in Auditorium F100, Yliopistokatu 7, Joensuu, on June 28th 2017, at 12 o'clock noon.

ISBN: 978-952-61-2540-4 (nid.)
ISBN: 978-952-61-2541-1 (pdf)
ISSN: 2242-1033

Grano Oy
Jyväskylä 2017

Abstract

Plastics, consisting of polymers and different additives, are an irremovable part of our daily life. One of the most important group of synthetic polymers are polyolefins, a vast majority of which are produced using heterogeneous Ziegler–Natta catalysts. Besides the precursor of active Ti species and aluminum alkyl cocatalyst, $MgCl_2$ support and Lewis bases (electron donors) are the essential components of a modern Ziegler–Natta catalyst. Although the role of electron donors is not completely confirmed, their coordination to $MgCl_2$ is known to be crucial, as electron donors can dictate the structure of $MgCl_2$ support and affect the properties of active polymerization sites. Comprehensive understanding of these effects would allow a more rational catalyst development.

In this study, the roles of multidentate ether and amine electron donors in the crystal structure formation of magnesium chlorides were studied using experimental and computational approaches.1,3-Dimethoxypropane, a simple diether, was unexpectedly found to be cleaved, when used as an electron donor in Grignard–Wurtz synthesis of a magnesium chloride-electron donor complex. The two-step cleavage reaction of diether is induced by a Grignard reagent and results in the formation of methoxymagnesium chloride (MgCl(OMe)). Diether acts as a source of methoxy groups in the reaction. Combined experimental and theoretical results indicate that MgCl(OMe) possesses a layered structure similar to that of $MgCl_2$. Calculations indicate a thermodynamic feasibility of the MgCl(OMe) formation and suggest an energetic preference for MgCl(OMe) to be structurally composed of alternating $MgCl_2$ and $Mg(OMe)_2$ stripes. Coordination of ester electron donors on MgCl(OMe) is weaker than on $MgCl_2$, whereas coordination of $TiCl_4$ is stronger in the case of methoxymagnesium chloride. MgCl(OMe)-$TiCl_4$ catalyst exhibited a high activity in ethylene polymerization, highlighting the potential of MgCl(OMe) as a support material for Ziegler–Natta type polymerization catalyst.

Crystalline magnesium chloride-electron donor complexes were formed in recrystallization of δ-$MgCl_2$ from excess of electron donor. The recrystallization products were identified as $[MgCl_2$(1,2-dimethoxyethane)$]_n$, $[Mg_2Cl_4$(1,3-dimethoxypropane$)_2(H_2O)]$ and $[MgCl_2$(*N*,*N*'-diethylethylenediamine$)_2]$ complexes. Crystal structures of the obtained complexes provide detailed information about the bonding of chelating electron donors in $MgCl_2$ supports. A possible formation of crystalline complexes must be considered when preparing Ziegler–Natta catalysts or modelling electron donor coordination on magnesium chlorides.

Polyethylenimines (PEIs), polymers bearing amino functionalities, were introduced as a new type of internal electron donors for Ziegler–Natta catalysts. A major advantage of PEIs with respect to conventional electron donors is their relative harmlessness. Both experimental and theoretical results indicate a strong coordination ability of branched PEI to $MgCl_2$. Based on computations, the structural variations in PEIs significantly affect their ability to stabilize the lateral surfaces of $MgCl_2$. PEIs seem to favor coordination on the $MgCl_2$ (110) surface and the coordination is especially strong in the case of branched PEIs. The performance of $MgCl_2$-PEI-$TiCl_4$ catalyst in the copolymerization of ethylene and 1-butene was good, indicating the potential of PEIs as internal electron donors for Ziegler–Natta catalysts. In conclusion, the results obtained in the study clarify the different roles of ether and amine electron donors in the crystal structure formation of magnesium chlorides. Furthermore, a new potential support material and internal electron donor for Ziegler–Natta type polymerization catalyst were introduced.

List of original publications

This dissertation is a summary of original publications **I-III** and submitted manuscript **IV**.

I Nissinen, V.; Pirinen, S.; Pakkanen, T. T. Unexpected Cleavage of Ether Bonds of 1,3-Dimethoxypropane in Grignard–Wurtz Synthesis of a $MgCl_2$–Donor Adduct. *J. Mol. Catal. A: Chem.* **2016**, *413*, 94–99.

II Nissinen, V. H.; Linnolahti, M.; Pakkanen, T. T. Methoxymagnesium Chloride – Structure and Interaction with Electron Donors: Experimental and Computational Study. *J. Phys. Chem. C* **2016**, *120*, 21505–21511.

III Nissinen, V. H.; Koshevoy, I. O.; Pakkanen, T. T. Crystalline Magnesium Chloride-Electron Donor Complexes: New Support Materials for Ziegler–Natta Catalysts. *Dalton Trans.* **2017**, *46*, 4452–4460.

IV Nissinen, V. H.; Linnolahti, M.; Bazhenov, A. S.; Pakkanen, T. T.; Pakkanen, T. A.; Denifl, P.; Leinonen, T.; Jayaratne, K.; Pakkanen, A. Polyethylenimines – Multidentate Electron Donors for Ziegler–Natta Catalysts. *Submitted for publication.*

The author's contribution to aforementioned publications:

The key ideas for the topics in Publications **I-IV** are based on conversations between the author and coauthors. The author carried out all the experimental work except the gas chromatography analyses in Publication **I,** the single-crystal X-ray structure determinations in Publication **III**, and the polymerizations and characterization of polymer products in Publication **IV**. In addition, the author carried out the cluster model calculations in Publication **II**. Manuscripts of publications **I–IV** were mainly written by the author.

Contents

Abstract **3**
List of original publications **4**
Contents **5**
Abbreviations **6**
1. Introduction **7**
1.1. $MgCl_2$ as a support for Ziegler–Natta catalyst 8
1.2. Other support materials for Ziegler–Natta catalyst 9
1.3. Electron donors 9
1.3.1. Diethers as electron donors 10
1.3.2. Polymeric electron donors 11
1.4. Crystalline magnesium chloride-electron donor complexes 11
1.5. Ethylene polymerization 12
1.6. Aims of the study 13
2. Experimental **15**
2.1. General considerations 15
2.2. Preparation of supports and precatalysts 15
2.2.1. Synthesis of magnesium chloride supports 15
2.2.2. Addition of electron donors and $TiCl_4$ to magnesium chloride supports 15
2.2.3. Synthesis of crystalline magnesium chloride-electron donor complexes 15
2.2.4. Preparation of $MgCl_2$-PEI-$TiCl_4$ precatalyst 16
2.3. Characterization of supports and precatalysts 16
2.4. Polymerizations 17
2.5. Computational details 17
3. Results and discussion **18**
3.1. Diethers as electron donors in Grignard–Wurtz synthesis of $MgCl_2$ 18
3.1.1. Ether cleavage during Grignard-Wurtz synthesis 19
3.1.2. Structure of MgCl(OMe) 22
3.1.3. MgCl(OMe) as a support material 24
3.1.4. Polymerization catalyst supported on MgCl(OMe) 28
3.2. Crystalline magnesium chloride-electron donor complexes 28
3.2.1. Magnesium chloride-1,2-dimethoxyethane complex 28
3.2.2. Magnesium chloride-1,3-dimethoxypropane complex 30
3.2.3. Magnesium chloride-*N,N'*-diethylethylenediamine complex 32
3.3. Polyethylenimines as electron donors for Ziegler–Natta catalysts 34
3.3.1. Interaction of PEI with $MgCl_2$ 34
3.3.2. Polymerization catalyst with PEI as internal electron donor 39
4. Conclusions **40**
Acknowledgements **42**
References **43**

Abbreviations

CP/MAS	cross polarization/magic angle spinning
DEEDA	*N*,*N*'-diethylethylenediamine
DFT	density functional theory
DIBP	diisobutyl phthalate
DME	1,2-dimethoxyethane
DMP	1,3-dimethoxypropane
DRIFT	diffuse reflectance infrared Fourier transform
EB	ethyl benzoate
EDTA	ethylenediaminetetraacetic acid
GGA	generalized gradient approximation
IR	infrared
M06-2X	meta-hybrid generalized gradient approximation functional of Zhao and Truhlar
NMR	nuclear magnetic resonance
PE	polyethylene
PEI	polyethylenimine
PXRD	powder X-ray diffraction
TEA	triethylaluminum
TZVP	triple-ζ-valence + polarization
XRD	X-ray diffraction

1. Introduction

Are we living in Plastic Age? Periods of human history have been defined based on materials and technologies that have affected most the society. Because plastics have such an important role in our everyday life, it is reasonable to argue that we truly are living in Plastic Age. Since the discovery of first fully synthetic polymer, Bakelite, in 1900s, a vast number of plastic materials, consisting of synthetic or semi-synthetic polymers and different additives, have been developed.[1] Due to their lightness, versatility, and processability, plastics have replaced many traditional materials in a large variety of applications, ranging from packaging and automotive industry to artificial joints.[1] The growing human population and rising standards of living have, nevertheless, challenged scientists to develop more and more efficient polymerization processes and better polymer products. A constant production of high-quality plastics is essential, if we are to maintain our modern lifestyle.

Polyethylene and polypropylene are among the most produced synthetic polymers, thus, possessing a vast commercial significance.[2,3] Majority of these two polyolefins are produced using heterogeneous Ziegler–Natta catalysts.[2] The history of Ziegler–Natta catalysis began in 1950s, when Karl Ziegler discovered that $TiCl_4$ combined with an aluminum alkyl polymerized ethylene in low pressures and temperatures, resulting in highly crystalline linear polyethylene.[3,4] Before this, polyethylene was produced in a high-pressure and high-temperature process, leading to branched polymers with different physical properties.[4] Shortly after Ziegler's discovery, Giulio Natta found that $TiCl_4/AlR_3$ catalyst was also able to produce isotactic polypropylene, starting the era of stereoregular polyolefins.[3] Since Ziegler's and Natta's discoveries, Nobel Prize worth in 1963, numerous studies have been conducted in order to improve the performance of the Ziegler–Natta catalysts and properties of the polymer products.[5] Major breakthroughs in the field have been immobilization of active titanium species on inorganic $MgCl_2$ support and introduction of Lewis bases (electron donors) to the catalytic system, resulting in notably enhanced activities and also improved stereoselectivity for propylene polymerization.[2,5] Especially in the last few decades, researchers have also focused on obtaining fundamental understanding of the catalytic system.[5,6] The development of computational methods has played an important role in the mechanistic studies.

Modern Ziegler–Natta catalysts are composed of a precursor of active Ti species ($TiCl_4$), supported usually on $MgCl_2$, and an aluminum alkyl cocatalyst, enabling polymerization by activating Ti centers through reduction and alkylation reactions.[5,7,8] Typically Ziegler–Natta catalysts also contain two types of Lewis bases.[5] An internal electron donor forms together with $TiCl_4$ and $MgCl_2$ support a precatalyst, which is activated with the cocatalyst in the presence of an external donor.[5] As a result of decades of intensive research, modern Ziegler–Natta catalysts exhibit high activities and good stereoregulating properties.[5] However, the research has so far mostly relied on trial and error, because there is still no profound understanding on the operation of the catalytic system.[9] For example, the exact structure of active sites and the role of electron donors are still not fully known. Solving these issues would allow a more rational development of catalysts with new and enhanced features. Furthermore, arisen health concerns associated with the use of certain plastic products and stricter regulation of chemicals have led to a need to find alternatives for conventional electron donors.[9–11] These are examples of the problems, which motivate researchers around the world to continue studying this intriguing catalytic system.

1.1. $MgCl_2$ as a support for Ziegler–Natta catalyst

Conventionally the role of support material is to disperse the active component over a large surface area, thus increasing the activity. The role of $MgCl_2$ support in Ziegler–Natta catalysis is more complex and $MgCl_2$ has been proposed to participate in the formation of active polymerization sites.[12] In fact, the use of $MgCl_2$ support increases both the number of catalytically active sites and their activities.[13] The crystal structure of $MgCl_2$ is composed of Cl–Mg–Cl triple layers packed in a lattice. The triple layers can be packed in a way that Cl atoms form a distorted cubic close-packed structure (α-$MgCl_2$) or a hexagonally close-packed structure (β-$MgCl_2$) (**Figure 1**).[14–16] When used as a support, $MgCl_2$ is usually in its activated form. This δ-$MgCl_2$ is characterized by a high structural disorder of Cl–Mg–Cl layers, a high number of unsaturated lateral surfaces, and a small crystallite size.[5,17,18] The suitability of $MgCl_2$ as a support material for active Ti species can be accounted for the similar crystal structures and lattice parameters of δ-$MgCl_2$ and δ-$TiCl_3$.[4] The lateral cuts of $MgCl_2$ exposing unsaturated Mg atoms are especially important, since they allow $MgCl_2$ to perform its role as a support by enabling coordination of active titanium species and electron donors.[13] **Figure 2** presents the catalytically relevant (104) and (110) surfaces, which possess 5- and 4-coordinated Mg atoms, respectively, in comparison to 6-coordinated Mg atoms of the bulk.[19,20]

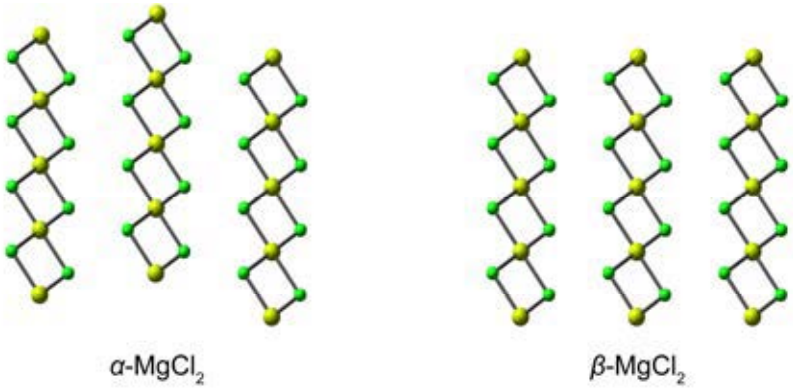

Figure 1. The packing of Cl–Mg–Cl triple layers in the polymorphic modifications of $MgCl_2$. Green = Cl, yellow = Mg.

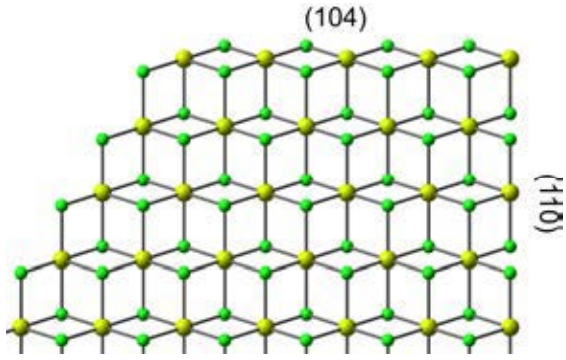

Figure 2. The structure of a single $MgCl_2$ layer presenting the catalytically relevant (104) and (110) surfaces. Green = Cl, yellow = Mg.

δ-$MgCl_2$ can be prepared by using mechanical or chemical activation methods or a combination of them.[5,21] In mechanical activation methods, ordered $MgCl_2$ is grounded typically in a ball mill.[22] $TiCl_4$ or Lewis bases can be added to the mixture in order to achieve even higher disorder.[5] The most commonly used chemical method involves preparation of $MgCl_2$-Lewis base (e.g. ethanol) adducts.[5] The removal of Lewis base by thermal or chemical treatment results in highly disordered $MgCl_2$.[23] Another chemical route to activated $MgCl_2$ utilizes Grignard and Wurtz coupling reactions (**Scheme 1**).[21,24] In this simple one-step method, magnesium metal reacts with *n*-alkyl chloride producing δ-$MgCl_2$, which exhibits a high degree of disorder, but also contains a minor amount of alkyl magnesium compounds.[21] The mechanical activation methods have been widely replaced by the chemical methods, because they produce δ-$MgCl_2$ with a higher degree of disorder and also enable better control over the particle morphology.[5,21]

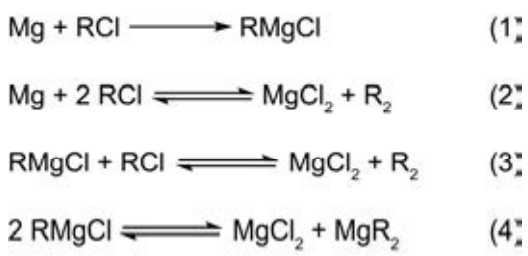

Scheme 1. Reactions of Grignard–Wurtz coupling. Reaction (1) describes Grignard reaction, reactions (2) and (3) Wurtz coupling reactions, and reaction (4) Schlenk equilibrium.

1.2. Other support materials for Ziegler–Natta catalyst

Since its discovery, $MgCl_2$ has been by far the most studied and utilized support material in Ziegler–Natta catalysts, as $MgCl_2$-supported catalysts have proven to possess the highest activities and best stereoselectivities.[5] However, there are also other potential support materials, including e.g. $MgBr_2$,[5] $MnCl_2$,[5] polymers,[25–27] SiO_2[28,29] and magnesium alkoxides ($Mg(OR)_2$)[30]. Alkoxymagnesium chlorides (MgCl(OR)) are another interesting, yet rarely studied group of support materials. Synthetic pathways leading to alkoxymagnesium chlorides and their use as precursors or components of Ziegler–Natta catalysts have been reported, indicating their potential as support materials.[31–39] However, no studies on the structures of alkoxymagnesium chlorides or their interaction with electron donors and $TiCl_4$ have been published.

1.3. Electron donors

Electron donors are Lewis bases, which can dictate the crystal structure of $MgCl_2$ by forming either a surface or a molecular complex with it.[40–43] Interaction of $MgCl_2$ with electron donors and $TiCl_4$ has been extensively studied using both experimental and computational approaches. The role of electron donors in the formation of $MgCl_2$ crystallites is important, as they can stabilize $MgCl_2$ crystals by coordinating on the unsaturated surfaces.[14,40,44–46] Electron donors can thus promote the formation of small $MgCl_2$ crystallites that is important for the activation of

$MgCl_2$.[44] Furthermore, in some cases electron donors can direct the growth of $MgCl_2$ nanocrystals by selectively stabilizing certain lateral surfaces.[15,43,47–52] In the absence of an electron donor, the (104) surfaces with weaker Lewis acidities are predominating, but the presence of an electron donor can make the formation of the (110) surfaces preferred.[19,46,47,50,53] It must be noted that surfaces in a real crystal are not always perfect, but may contain different types of surface defects, including e.g. steps and kinks.[54] The surface defects complicate the situation by highly increasing the number of possible coordination sites.[55–57] Some typical electron donors used in Ziegler–Natta catalysts are presented in **Figure 3**.

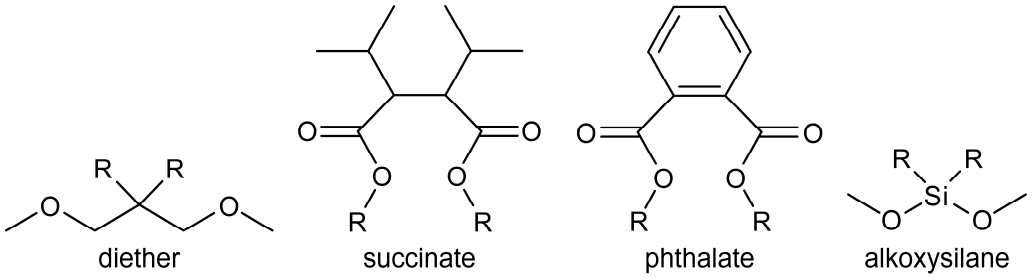

Figure 3. Typical electron donors used in Ziegler–Natta catalysts. R represents an alkyl group.

Although the role of electron donors in the polymerization process is not completely confirmed, it is evident that they play a key role. Electron donors significantly affect the properties of both the catalyst (e.g. activity, stereoselectivity, hydrogen response) and polymer product (e.g. molar mass, molar mass distribution, tacticity).[5,6,13,45,58,59] Previously, it was assumed that the main function of electron donors was to control the amount and distribution of active titanium species in the catalyst. $TiCl_4$ can form either a mononuclear ($TiCl_4$) or a binuclear (Ti_2Cl_8) species on the lateral $MgCl_2$ surfaces.[5] Electron donors were assumed to hinder the formation of less stereoselective Ti species by selectively coordinating on the (110) surface.[59] The precursor of stereoselective active species was assumed to be Ti_2Cl_8 dimer coordinated on the (104) surface of $MgCl_2$.[58,59] However, the latest experimental and theoretical studies have indicated the instability of dimeric titanium species on the (104) surface.[60] According to the current understanding, the role of electron donors is rather to modify the local environment of active titanium species by coadsorbing to their proximity.[13,61–63] The precursor of active species is assumed to be mononuclear $TiCl_4$ coordinated on the (110) (or alike) surface.[28,50,60,64,65] Furthermore, computational results by Credendino et al. suggest that the active titanium species could be located also on the defected (104) surface.[57]

1.3.1. Diethers as electron donors

Diethers are industrially important bidentate electron donors bearing two ether groups (see **Figure 3**). Uniquely, Ziegler–Natta catalysts with diether electron donors exhibit a high activity in stereoselective polymerization of propylene, even in the absence of an external electron donor.[5] In addition, these catalysts usually exhibit a high hydrogen response and good stability under the polymerization conditions.[6,66,67] The distance between coordinating atoms of a bidentate electron donor has been proven to be a key factor in binding to $MgCl_2$.[6,68] 1,3-Diethers have been found to possess suitable oxygen–oxygen distances for coordination to $MgCl_2$ (approximately 2.8–3.2

Å) and, thus, are commonly utilized as electron donors.[6,68] According to theoretical studies, diethers prefer a chelate binding mode.[45,62,69] Furthermore, both experimental and computational studies have shown that diethers preferably coordinate on the (110) surface of $MgCl_2$.[5,41,45,49,70]

1.3.2. Polymeric electron donors

Polymeric compounds bearing suitable functionalities (e.g. ether groups) can be used as electron donors in Ziegler–Natta catalysts. Although polymers are interesting and potential alternatives for conventional electron donors, they have not yet drawn much attention. Only the use of certain polyethers (e.g. polyethylene glycols and polytetrahydrofurans) has been reported in the field of Ziegler–Natta catalysis.[71–73] Interaction of polyethylene glycol with $MgCl_2$ has been more extensively studied in the context of electrolytes.[24,74,75] It can be assumed that the binding properties of a polymeric electron donor are strongly influenced by the structural features (e.g. the distance between electron donating atoms, polymer chain length, and branching). Hence, the structural adjustments may offer a way to tailor the electron donating properties of a polymeric donor suitable for various applications.

1.4. Crystalline magnesium chloride-electron donor complexes

In addition to the surface complex formation described above, electron donors can form also molecular complexes with $MgCl_2$. These magnesium chloride-electron donor complexes can be considered as crystalline models, which provide detailed information about the bonding and coordination modes of electron donors in $MgCl_2$ supports. In addition, the crystal structures of these complexes can provide further insight into the role of electron donors in the formation of crystalline $MgCl_2$ phases.[16,76] For example the industrially important $MgCl_2$-ethanol adducts ($MgCl_2$·nEtOH), which are often employed in the preparation of Ziegler–Natta catalysts, have been thoroughly studied.[23,77–82] Although ethanol is removed during the support preparation, the initial composition and architecture of $MgCl_2$-ethanol adduct affects the properties of the final catalyst, making the structural information highly important.[76,77] Certain $MgCl_2$-ethanol adducts have been found to possess polymeric structures.[77] It has been proposed that the nanoporosity and high surface area of chemically activated δ-$MgCl_2$ results from the formation of these polymeric $MgCl_2$-electron donor complexes, which retain their structural framework despite the removal of electron donor.[76,77] $MgCl_2$ complexes with other alcohols have been studied, as well.[83–87]

In addition to alcohols,[77–79,86] the syntheses and crystal structures of magnesium chloride complexes with various other electron donors, including e.g. tetrahydrofuran,[88–90] alkyloxy ethanols,[91,92] pyridine,[93] esters,[94,95] and ketones[96] have been reported. Also the crystal structures of magnesium bromide complexes with ethers have been published.[97–99] Despite the high industrial relevance of diether electron donors, the syntheses and crystal structures of magnesium chloride-diether complexes have been rarely reported.[100] Crystalline magnesium chloride complexes with other electron donors besides ethanol can also be used as components of Ziegler–Natta catalysts, as Di Noto et al. and Pirinen et al. have demonstrated.[101,102]

1.5. Ethylene polymerization

Polyethylene (PE) is a simple polymer having the chemical formula $(C_2H_4)_n$. Polyethylene is mainly produced using heterogeneous catalysis, most notably with Ti-based Ziegler–Natta catalysts.[103] The physical properties of PE depend on the structural features (e.g. molar mass and molar mass distribution),[104,105] which are highly dependent on the properties of the catalyst utilized. For example the physical properties of catalyst particles (size, porosity, surface area), the local environment of active sites, and the possible presence of electron donors are known to have an influence on the properties of the final catalyst.[40,106–109] Furthermore, the polymerization conditions also affect the properties of polymer produced.[110] Particular attention must thus be paid during both the catalyst preparation and polymerization in order to obtain polymer with desired properties.

Active sites of a Ziegler–Natta catalyst are typically heterogeneous (multi-site catalyst) that results in widening of the molar mass distribution.[109–112] The presence of an electron donor usually decreases the activity of the catalyst in ethylene homopolymerization, but increases the molar mass and narrows down the molar mass distribution of the polymer product.[6] Similarly, the presence of hydrogen, which is used to adjust the molar mass, decreases the activity of the catalyst.[6,108]

Addition of α-olefin (comonomer, e.g. 1-butene) into the reaction mixture during the polymerization of ethylene results in the formation of short chain branches to the polyethylene backbone chain. Branching significantly affects the physical properties (e.g. density, melting point, crystallinity, tensile properties) of the copolymer product. In suitable conditions, the polymer formed in such copolymerization is called linear low density polyethylene (LLDPE).[105] The ability of a catalyst to incorporate comonomers into a growing polymer chain is highly dependent on the nature of active sites.[113] The use of electron donors typically enhances the comonomer incorporation.[6] The addition of a comonomer into ethylene polymerization system is known to increases the rate of polymerization.[6,108] A plausible explanation to this so-called comonomer effect is the easier access of monomers to active sites.[114] Furthermore, the presence of α-olefin besides ethylene may increase the number of active sites due to activation of otherwise inactive centers or enhanced fragmentation of catalyst particles.[108,114] On the other hand, the presence of comonomers often decreases the molar mass of the polymer product.[6,108]

Although the nature of active polymerization sites is not completely confirmed, it is unanimously assumed that a Ti–C bond plays a key role in the polymerization process.[5] Formation of the active metal–carbon bond most probably results from alkylation reactions of Ti centers by aluminum alkyl cocatalyst during the catalyst activation.[5,7,8] Furthermore, considerable reduction of Ti centers from the initial oxidation state (+4) of $TiCl_4$ is likely to occur during the activation process, resulting in the formation of Ti^{3+} and even Ti^{2+} species.[5] The polymerization of ethylene by a Ti-based catalyst is generally accepted to proceed via Cossee–Arlman mechanism (**Scheme 2**).[4,105,115] The active site is assumed to be a Ti center coordinated by four chloride ligands and an alkyl group. The active site possesses also a coordination vacancy, where an ethylene molecule can coordinate. An insertion reaction of ethylene between titanium and the alkyl group follows. Meanwhile, a new vacant site is generated, enabling coordination of next ethylene monomer. Repetitive additions of ethylene molecules produce a polyethylene chain.[105] The most important

polymer chain termination mechanisms include a chain transfer with hydrogen molecule (molar mass modifier), monomer or cocatalyst.[108] In addition, the chain termination can also occur through β-hydride elimination.[108]

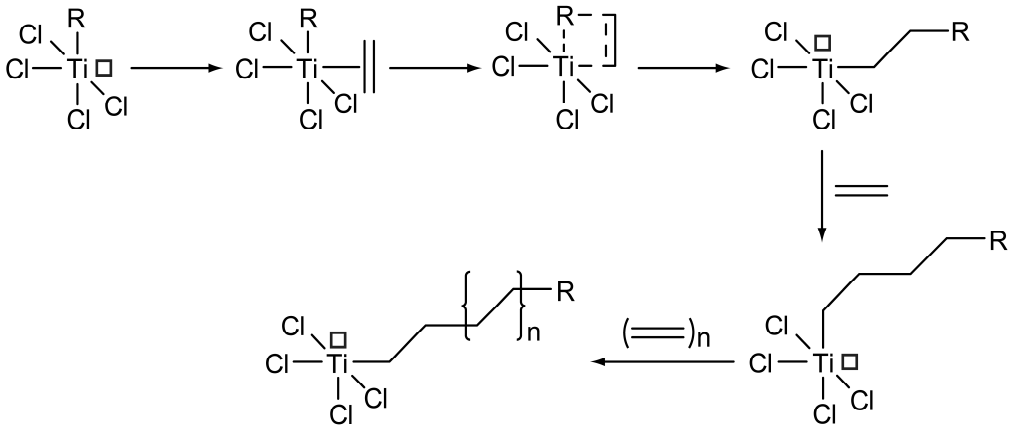

Scheme 2. Mechanism of ethylene polymerization using a transition metal catalyst. Black box represents a vacant coordination site.[105]

1.6. Aims of the study

This thesis focuses on supported, Ti-based Ziegler–Natta catalysts, some fundamental aspects of which are still unclear. As highlighted in the previous chapters, electron donors can dictate the structure of $MgCl_2$ support, which notably influences the properties of the catalytic system. The aim of the thesis is to study the effect of multidentate oxygen- and nitrogen-containing electron donors on the formation of magnesium chloride structures utilizing both experimental and computational approaches. Particular attention is paid to the interaction of electron donors with magnesium chloride-based support materials. Diethers are chosen as electron donors due to their industrial importance. In addition, their nitrogen-containing counterparts (diamines) are studied to obtain a more comprehensive understanding of coordination of chelating electron donors to magnesium chlorides. The electron donors included in the study are presented in **Figure 4**. The knowledge of electron donor influence on the structure of magnesium chlorides can be useful in the development and modelling of Ziegler–Natta polymerization catalysts.

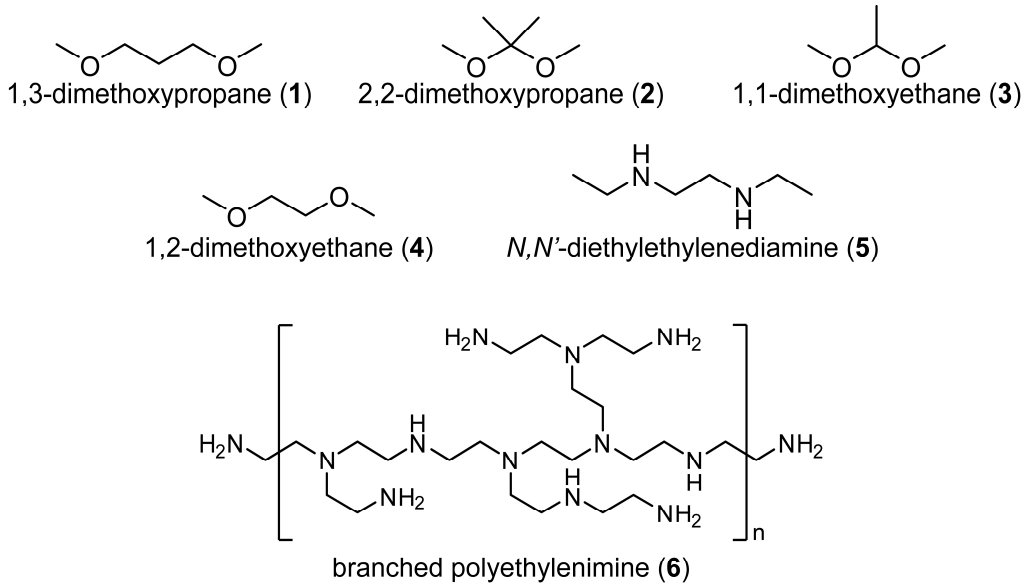

Figure 4. Structures of electron donors used in the study.

The effect of diethers on the structure of magnesium chlorides is studied using two different synthesis approaches. Firstly, magnesium chloride is synthesized in the presence of diether electron donors utilizing Grignard–Wurtz coupling reactions. Secondly, δ-$MgCl_2$ is recrystallized from excess of electron donor. The aim is to identify and characterize the reaction products and, thus, to clarity the roles of bidentate electron donors in the crystal structure formation of magnesium chlorides. Furthermore, the properties of the reaction products as support materials for a Ziegler–Natta type polymerization catalyst are of interest.

Suitable alternatives for conventional electron donors are constantly sought. An important criterion is that the new electron donors should be less harmful than the conventional donors. One goal of the thesis is to pursue an idea of using nitrogen-containing polymers (structure **6** in **Figure 4**) as novel multidentate electron donors for Ziegler–Natta catalysts.

2. Experimental

2.1. General considerations

Magnesium chloride supports and Ziegler–Natta catalysts are highly air-sensitive. Thus, the preparation of the supports and precatalysts and the handling of the samples were conducted strictly under a nitrogen or argon atmosphere using a glovebox and Schlenk techniques. The glassware and autoclave used in the experiments were dried in an oven at 110 °C and quickly transferred into the antechamber of the glovebox, when needed. The solvents and electron donors were dried using 3 Å molecular sieves, with the exception of branched polyethylenimine (M_w = 800 g/mol), which was dried under vacuum at 120 °C overnight. Some materials and reagents used in the experiments are highly pyrophoric and must be handled cautiously.

2.2. Preparation of supports and precatalysts

2.2.1. Synthesis of magnesium chloride supports

δ-$MgCl_2$ was synthesized according to a method presented by Di Noto et al. with minor modifications.[21] Magnesium, 1-chlorobutane (in a molar ratio of 1:3), a few small crystals of iodine and octane (solvent) were packed into an autoclave, which was heated at 130 °C for 2 h. The solid product formed in the reaction (fine white powder) was separated, washed with octane and dried under vacuum at room temperature.

Attempted syntheses of magnesium chloride-diether complexes were performed using the same synthesis method as in the case of δ-$MgCl_2$, but in the presence of a diether electron donor. A Mg/donor molar ratio of 2:1 was used.

2.2.2. Addition of electron donors and $TiCl_4$ to magnesium chloride supports

Addition of electron donors and $TiCl_4$ to magnesium chloride supports were conducted in an autoclave using toluene as the solvent medium. For the addition of electron donors, reagents were packed into an autoclave, which was heated at 130 °C for 2 h. The solid products were separated, washed with toluene and dried under vacuum. In the case of $TiCl_4$, the reaction temperature was 100 °C for 2 h and a Mg/Ti molar ratio of 1:10 was used. $TiCl_4$-containing products were washed with both toluene and heptane and dried under reduced pressure.

2.2.3. Synthesis of crystalline magnesium chloride-electron donor complexes

Crystalline magnesium chloride-electron donor complexes were prepared by recrystallization of δ-$MgCl_2$ in the presence of chelating electron donors. δ-$MgCl_2$ and a large molar excess of electron donor were packed into an autoclave. Reaction temperatures (50–130 °C) and times (3–14 days) were optimized for each electron donor in order to obtain large crystals of good quality. After the reaction, crystalline solids were detected on the bottom and walls of the autoclave (**Figure 5**). The liquid phase was removed and the solid product was dried under reduced pressure at room temperature.

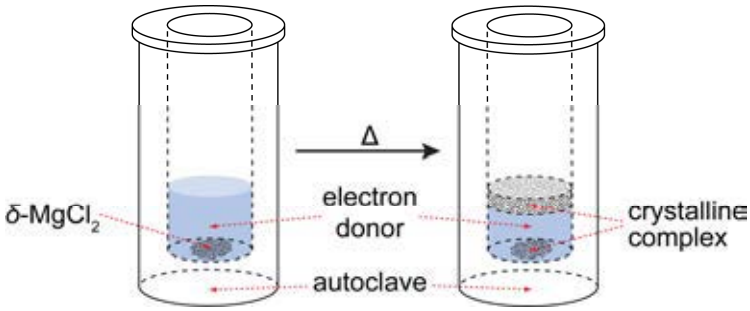

Figure 5. Schematic presentation of the recrystallization process in an autoclave.

2.2.4. Preparation of $MgCl_2$-PEI-$TiCl_4$ precatalyst

A precatalyst containing branched PEI as internal electron donor was prepared by a sequential addition of PEI and $TiCl_4$ to a $MgCl_2$-EtOH support[116–118]. First, PEI was added to a $MgCl_2$-EtOH adduct (a Mg/PEI molar ratio of 1.1) in an autoclave using toluene as the solvent medium (90 °C/22 h). Next, $TiCl_4$ was added to the separated and toluene-washed $MgCl_2$-EtOH-PEI support in a glass reactor. A slurry of support and heptane was cooled to 10 °C, followed by a slow addition of $TiCl_4$ (n(Ti):n(EtOH) = 5.5). After 30 min, temperature of the system was slowly raised to 110 °C. After 60 min of mixing at 110 °C, the solid product was separated and extensively washed using $TiCl_4$, toluene and heptane. The precatalyst obtained was dried under vacuum at room temperature. Further details of the precatalyst preparation are presented in Publication **IV**.

2.3. Characterization of supports and precatalysts

Powder X-ray diffractograms (PXRD) were recorded using Cu K_α radiation (λ = 1.5418 Å), a measurement range (2θ) of 4–70°, a step size of 0.05°, and a time per step of 8 s. The samples were protected from air by Mylar film. Single-crystal X-ray diffraction was utilized in the structure determinations of crystalline complexes. The air-sensitive crystals were protected from air by immersing them in Fomblin oil, mounted in a nylon loop, and measured at a temperature of 120 or 150 K using Mo K_α radiation (λ = 0.71073 Å). Further details of X-ray structure determinations are presented in Publication **III**.

^{13}C NMR spectra of the solid products were recorded using cross polarization and magic angle spinning (CP/MAS) and the following parameters: a spin rate of 4500 Hz, a relaxation delay of 5 s, a contact time of 3.0 ms and a number of scans of 10000. Glycine was used as an external reference. IR spectra of the solid samples were recorded in a DRIFT (diffuse reflectance infrared Fourier transform) mode using 32 scans and a resolution of 2 cm^{-1}.

The magnesium content of the solid products was determined by a complexometric EDTA (ethylenediaminetetraacetic acid) titration. The amounts of organic molecules and moieties in complexes were determined by ^1H NMR spectroscopy (a number of scans of 32 and a relaxation delay of 10 s). Solid products were dissolved in D_2SO_4/D_2O solution and sodium acetate was used

as an internal standard. The titanium content of the products was determined by a spectrophotometric method, in which solids were dissolved in H_2SO_4 solution and addition of H_2O_2 gave solutions of a yellow complex.[119] Absorbances of the solutions were read at 410 nm wavelength.

2.4. Polymerizations

For ethylene homopolymerizations, a precatalyst, triethylaluminum (TEA) cocatalyst (an Al/Ti molar ratio of 100:1), and heptane were packed into a 100 ml autoclave, which was heated to 50 °C. Pressure was maintained at a constant level (2.0 bar) by a continuous ethylene feed. The polymerization was terminated after 60 min by ventilation of ethylene gas.

Copolymerizations of ethylene and 1-butene were conducted in a 3-liter semibatch reactor using triethylaluminum as a cocatalyst (an Al/Ti molar ratio of 15:1). Propane, 1-butene and H_2 were added into the reactor, which was heated to reaction temperature (85 °C). An ethylene batch was introduced into the reactor, followed by catalyst and TEA. Constant pressure was maintained by a continuous ethylene feed. Polymerizations were stopped after 60 minutes by venting off monomers and H_2. Further details of the ethylene/1-butene copolymerizations are presented in Publication **IV**.

2.5. Computational details

All calculations were performed using Gaussian09 program package.[120] Both cluster models and periodic models of magnesium chlorides and their donor/$TiCl_4$ complexes were studied by the means of DFT (density functional theory) methods. M06-2X meta-hybrid GGA (generalized gradient approximation) functional[121] was chosen to be used in the calculations, based on benchmarking by Ehm et al.[122] Optimized triple-ζ-valence + polarization basis sets (TZVP), derived from the def-TZVP basis sets of Ahlrics and coworkers,[123] were used in all calculations. Further details of the quantum chemical calculations are presented in Publications **II** and **IV**.

3. Results and discussion

3.1. Diethers as electron donors in Grignard–Wurtz synthesis of $MgCl_2$

The effect of diether electron donors on the structure of $MgCl_2$, prepared utilizing Grignard–Wurtz coupling reactions, was studied by performing Grignard–Wurtz synthesis in the presence of 1,3-dimethoxypropane diether (structure **1** in **Figure 4**). Magnesium, 1-chlorobutane, and 1,3-dimethoxypropane (in a molar ratio of 2:6:1) were used as reactants and octane as the solvent medium (130 °C/2h). According to a PXRD study presented in **Figure 6**, the solid product formed was highly disordered, but unexpectedly it did not possess the typical characteristics of δ-$MgCl_2$. In fact, based on IR, CP/MAS ^{13}C NMR (**Figure 7**) and ^{1}H NMR spectroscopic data, the product was found to contain methoxy groups (OCH_3 = OMe) and a minor amount 1,3-dimethoxypropane. Based on ^{1}H NMR analysis and EDTA titrations, Mg/MeO and Mg/1,3-dimethoxypropane molar ratios were 1:0.82 and 1:0.047, respectively. The molar ratio of magnesium to chlorine was 1:1.26. As a conclusion, most of the 1,3-dimethoxypropane had been cleaved during the reaction and every mole of 1,3-dimethoxypropane produced approximately two moles of methoxy groups. The product formed in the reaction was most probably methoxymagnesium chloride (MgCl(OMe)), containing a minor amount of unreacted 1,3-dimethoxypropane. Formation of other alkoxymagnesium chlorides in similar reaction conditions from different sources of alkoxy groups has been previously reported.[31,32,35,39]

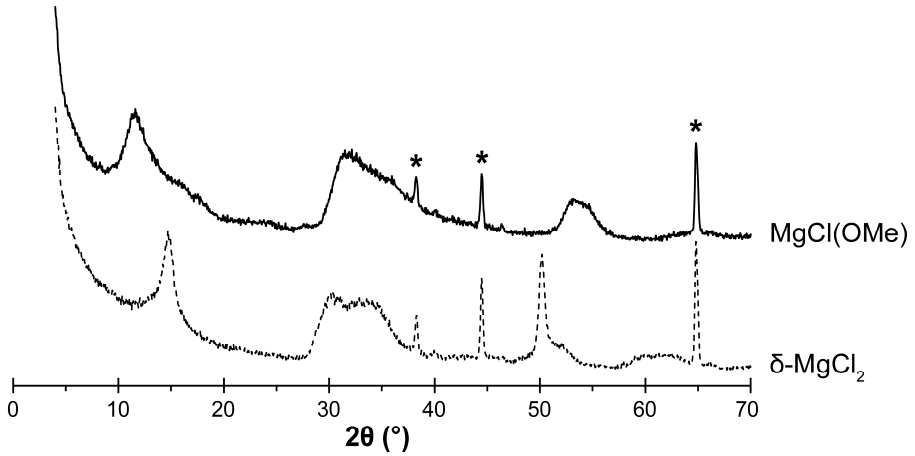

Figure 6. Powder X-ray diffractograms of the solid product from Grignard–Wurtz synthesis in the presence of 1,3-dimethoxypropane (MgCl(OMe); solid line) and δ-$MgCl_2$ (dashed line). Reflections of the sample holder are marked with asterisks (*).

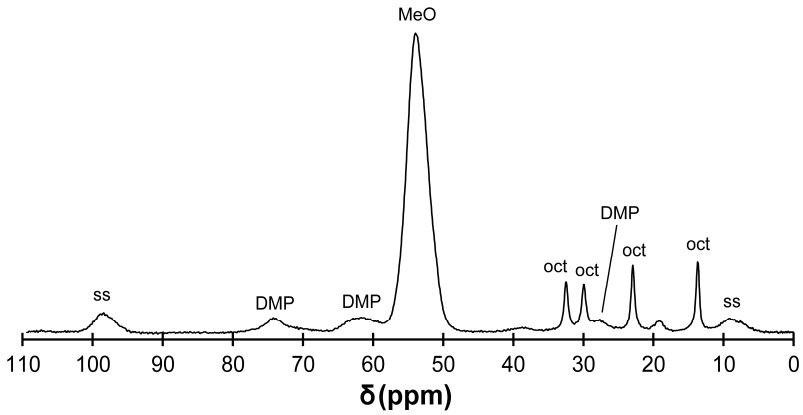

Figure 7. CP/MAS ^{13}C NMR spectrum of the solid product from Grignard-Wurtz synthesis in the presence of 1,3-dimethoxypropane as electron donor (MgCl(OMe)). MeO = methoxy group, DMP = 1,3-dimethoxypropane, oct = octane, ss = spinning sideband.

In addition to 1,3-dimethoxypropane, two other diethers, 2,2-dimethoxypropane and 1,1-dimethoxyethane (structures **2** and **3** in **Figure 4**), were studied as electron donors in Grignard–Wurtz synthesis using the same amounts of reactants and reaction conditions as in the case of 1,3-dimethoxypropane. Based on PXRD and spectroscopic data, the solid reaction products consisted mainly of methoxymagnesium chloride.

3.1.1. Ether cleavage during Grignard-Wurtz synthesis

The cause of ether cleavage during Grignard–Wurtz synthesis was studied by heating 1,3-dimethoxypropane in the presence of 1-chlorobutane or δ-$MgCl_2$ and using octane as the solvent medium. The cleavage reaction was not observed in either of these two cases, indicating that heat or the presence of δ-$MgCl_2$ was insufficient to decompose 1,3-dimethoxypropane in the reaction conditions (130 °C/2h). However, when commercial butylmagnesium chloride solution was added to a partly crystalline magnesium chloride-1,3-dimethoxypropane complex, prepared by addition of diether to prior-synthesized δ-$MgCl_2$, a partial cleavage of 1,3-dimethoxypropane was observed. Publication **I** includes further details. The result suggested that the Grignard reagent formed in Grignard–Wurtz coupling reactions (**Scheme 1**) was likely responsible for the cleavage reaction of diethers during Grignard–Wurtz synthesis.

In order to provide further insight into the reaction path of ether cleavage, Grignard–Wurtz synthesis in the presence of 1,3-dimethoxypropane was repeated in a glass reactor at atmospheric pressure using the same amounts of reagents and reaction temperature as in the case of autoclave synthesis. The experimental set-up enabled sampling during the course of the reaction and, thus, monitoring the progress of the reaction. The solid reaction products were separated, dissolved in D_2SO_4/D_2O solution, and analyzed by ^1H NMR. The results are summarized in **Figure 8**, where the amounts of 1,3-dimethoxypropane and methoxy groups in the solid products are presented as a function of the reaction time. In the beginning of the reaction, the solid magnesium product contained more 1,3-dimethoxypropane than methoxy groups. As the reaction proceeded, the amount of 1,3-dimethoxypropane decreased rapidly and simultaneously the amount of methoxy

groups increased. Diether most probably first binds to the solid magnesium product formed in the reaction, and later undergoes a cleavage reaction producing methoxy groups.

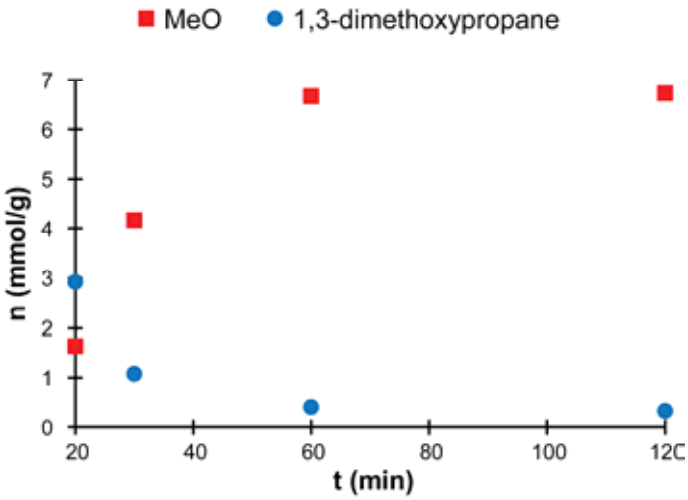

Figure 8. The molar amounts of MeO and 1,3-dimethoxypropane per gram of the solid product presented as a function of the reaction time. t = 0 corresponds to the starting time of the heating.

The liquid phase of the reaction mixture was also analyzed as a function of the reaction time (**Figure 9**). The liquid samples were diluted in $CDCl_3$ and analyzed by ^1H NMR. In the early stages of the reaction (t = 20 and 30 min), two new unsaturated compounds, identified as 3-methoxy-1-propene and 1-heptene, were found to be present in the liquid phase. As the reaction progressed, the amount of 3-methoxy-1-propene decreased, and in the end of the reaction (t = 120 min) there was virtually none left, whereas 1-heptene was still present. The results suggest that the cleavage reaction of 1,3-dimethoxypropane probably first produces 3-methoxy-1-propene intermediate, which reacts further producing 1-heptene. In both steps one methoxy group is cleaved, resulting eventually in the formation of methoxymagnesium chloride. Analysis of the gas phase of the reaction mixture (t = 120 min) by IR spectroscopy and gas chromatography revealed another possible terminal alkene by-product, likely propene. The two observed by-products indicate the existence of at least two parallel reaction paths for the diether cleavage.

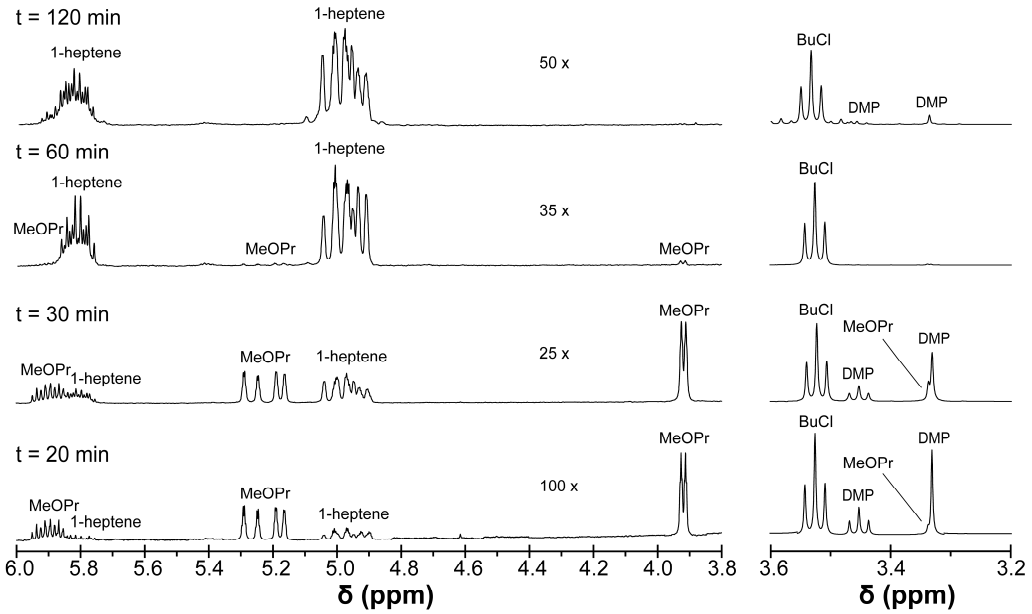

Figure 9. ^{1}H NMR spectra of the liquid phase of the reaction mixture from Grignard–Wurtz synthesis in the presence of 1,3-dimethoxypropane at different intervals from the beginning of the reaction. Regions 3.8–6.0 ppm and 3.2–3.6 ppm are presented on a different intensity scale. t = 0 corresponds to the starting time of the heating. MeOPr = 3-methoxy-1-propene, BuCl = 1-chlorobutane, DMP = 1,3-dimethoxypropane.

The probable intermediate product 3-methoxy-1-propene was also studied as an electron donor in Grignard-Wurtz synthesis using the same reaction conditions as in the case of 1,3-dimethoxypropane (a Mg/donor molar ratio of 2:1). Spectroscopic data indicated the presence of methoxy groups in the solid magnesium product. According to a PXRD study, the reaction product was a mixture of MgCl(OMe) and $MgCl_2$ phases due to high magnesium/methoxy molar ratio of 2:1 used in the synthesis. The analyses of the gas and liquid phases of the reaction mixture confirmed the formation of 1-heptene and propene by-products also in this case. The experiment provided further support for 3-methoxy-1-propene being an intermediate product of the cleavage reaction of 1,3-dimethoxypropane during Grignard–Wurtz synthesis.

A possible reaction path for the cleavage of 1,3-dimethoxypropane resulting in the formation of 1-heptene as a by-product is presented in **Scheme 3**. First step in the reaction path is an elimination of OCH_3 induced by a strong nucleophile BuMgCl.[124] 3-Methoxy-1-propene is produced in the reaction along with methoxymagnesium chloride and butane, which is formed via a *β*-hydrogen abstraction. Second step in the reaction path involves a OCH_3 substitution of 3-methoxy-1-propene intermediate by butyl anion of BuMgCl. There are two possibilities how the carbanion can attack 3-methoxy-1-propene, namely 1,2-addition and 1,4-addition.[125,126] Both ways result in the formation of methoxymagnesium chloride and 1-heptene.

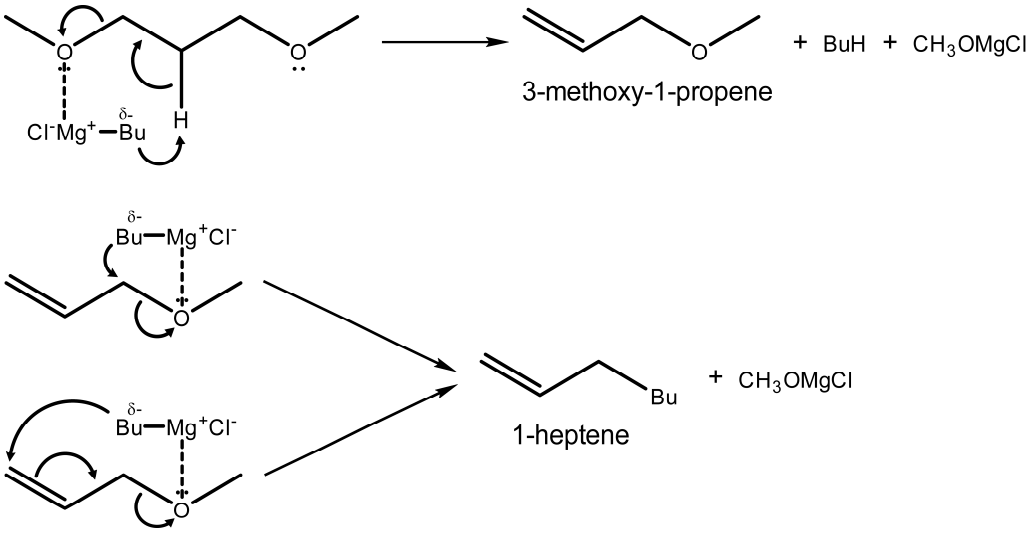

Scheme 3. A proposed reaction path for the cleavage reaction of 1,3-dimethoxypropane by Grignard reagent, resulting in the formation of 1-heptene as a by-product.

The formation of propene, another observed by-product, has been reported in the cleavage of allylic ethers.[126] Kharasch et al. have studied the cleavage reactions of ethers by Grignard reagents in the presence of metal halides.[127–131] Propene formation was reported in the cleavage of phenyl allyl ether by Grignard reagent in the presence of cobalt chloride. Furthermore, Ohkubo et al. have reported the cleavage of allylic ethers in the presence of a low-valent titanium species, magnesium chloride and magnesium metal.[132] The reaction was proposed to result in the formation of methoxy ion and allyl anion or allyl radical. Based on these literature results, heating of 3-methoxy-1-propene was studied in the presence of magnesium metal and δ-$MgCl_2$ using octane as the solvent medium (130 °C/2h). ^{1}H NMR analysis of the solid product dissolved in D_2SO_4/D_2O solution revealed partial cleavage of 3-methoxy-1-propene, indicating that the presence of magnesium and δ-$MgCl_2$ can cause the cleavage reaction even in the absence of a Ti species. Analysis of the gas phase of the reaction mixture indicated possible presence of propene, whereas 1-heptene was not found to be present in the liquid phase of the reaction mixture.

3.1.2. Structure of MgCl(OMe)

According to a PXRD study presented in **Figure 6**, methoxymagnesium chloride formed in Grignard–Wurtz synthesis possesses a diffraction pattern similar to that of δ-$MgCl_2$ prepared with the same synthesis method, but in the absence of an electron donor. The congruence between X-ray patterns indicate that methoxymagnesium chloride possesses a layer structure similar to that of δ-$MgCl_2$. The signals of MgCl(OMe) are wider than the signals of δ-$MgCl_2$, indicating even a higher structural disorder or a smaller crystallite size. Furthermore, a broad signal of methoxy groups in the CP/MAS ^{13}C NMR spectrum (**Figure 7**) at 54 ppm, as well as the broad absorption of C–O stretching vibration in the IR spectrum at 1000 cm^{-1} indicate multiple possible chemical environments of methoxy groups in MgCl(OMe).

Computational approach was employed together with experimental methods in order to provide further insight into general structural features of MgCl(OMe). To make a comparison to analogous $MgCl_2$ and $Mg(OMe)_2$ structures, cluster of up to four MgCl(OMe) monomers were studied in all possible configurations. The most stable MgCl(OMe) tetramer obtained closely resembles the $MgCl_2$ tetramer (**Figure 10**).[133] The preferable distribution of methoxy groups in the structure of MgCl(OMe) was studied by increasing the size of the cluster to construct a hexagonal structure[46] of 19 monomers and by altering the mutual arrangement of methoxy groups. The most stable configuration (see **Figure 10**) shows that the methoxy groups favor positions close to each other, resulting in the formation of alternating $Mg(OMe)_2$ and $MgCl_2$ stripes. Furthermore, an energy comparison between $MgCl_2$, $Mg(OMe)_2$, and MgCl(OMe) clusters (**Table 1**) indicated a thermodynamic feasibility for the formation of methoxymagnesium chloride.

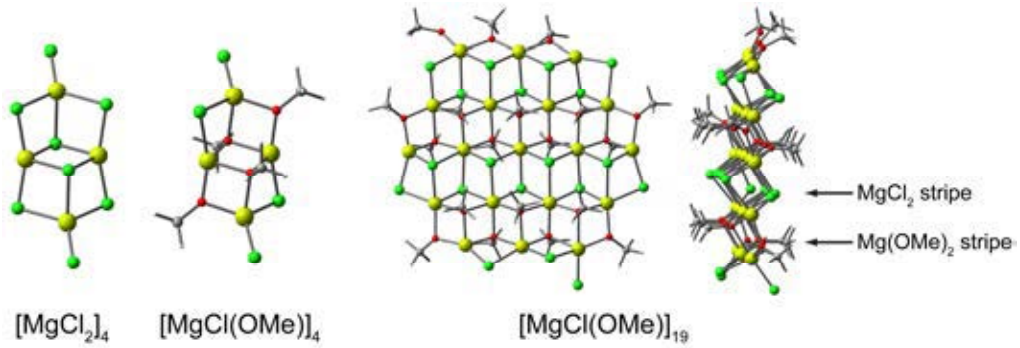

Figure 10. The most stable tetrameric $[MgCl_2]_4$ and $[MgCl(OMe)]_4$ structures and a hexagonal structure of $[MgCl(OMe)]_{19}$ cluster viewed from two different orientations. Green = Cl, yellow = Mg, red = O, gray = C.

Table 1. Energy (ΔE/Mg) and Gibbs energy (ΔG/Mg) for the reaction $[MgCl_2]_x + [Mg(OMe)_2]_x \rightleftharpoons 2\ [MgCl(OMe)]_x$ as a function of the cluster size.

x	ΔE/Mg (kJ/mol)	ΔG/Mg (kJ/mol)[a]
1	–3.8	–10.7
2	–43.0	–41.5
3	–31.0	–30.0
4	–39.7	–38.0
19	–22.1	–22.0

[a]Gibbs energies were calculated at T = 298 K and p = 1 atm.

A systematic study of MgCl(OMe) monolayer systems was conducted using periodic models in order to verify the structure proposed by cluster calculations and to generalize the structural features to analogous crystallites. The layers were described by a multiplication of a $Mg_4Cl_x(OMe)_y$ supercell, where $x + y = 8$. The most stable structure was obtained at equivalent

composition Cl:OMe = 1:1 (x = y = 4), suggesting, in accordance with the cluster model calculations, a preferable mixing of Cl and OMe units giving MgCl(OMe). In an optimized structure, $MgCl_2$ and $Mg(OMe)_2$ units are arranged in a form of alternating stripes (**Figure 11**). The energy of MgCl(OMe) with respect to pure $MgCl_2$ is –48.3 kJ/mol per each Mg atom. However, it is unlikely that the synthesized methoxymagnesium chloride possesses this neatly ordered structure throughout the whole material. Most probably the product possesses, in addition to layer stacking disorder, also intralayer disorder between Cl and OMe units, which would in part explain the observed high disorder in PXRD.

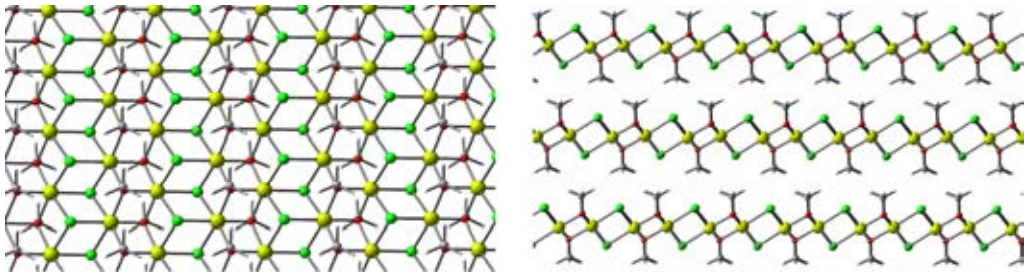

Figure 11. The structure of a single MgCl(OMe) layer viewed from orientation parallel to the basal (100) surface (left) and multilayer structure of MgCl(OMe) (right) based on periodic quantum chemical calculations. Green = Cl, yellow = Mg, red = O, gray = C.

3.1.3. MgCl(OMe) as a support material

The properties of methoxymagnesium chloride as a support material for Ziegler–Natta type polymerization catalyst were of interest. Hence, interaction of typical ester electron donors and $TiCl_4$ with MgCl(OMe) was studied by adding diisobutyl phthalate (DIBP), ethyl benzoate (EB), and $TiCl_4$ to MgCl(OMe). A Mg/donor molar ratio of 1:1 and a Mg/Ti molar ratio of 1:10 were used. Chemical compositions of the reaction products are presented in **Table 2**. The amounts of electron donors in MgCl(OMe)-donor complexes are low compared to similar $MgCl_2$-donor complexes,[15,43] whereas the Ti content of MgCl(OMe)-$TiCl_4$ complex is of same order as in the case $MgCl_2$-$TiCl_4$ complex. Based on a PXRD analysis, introduction of ester electron donors or $TiCl_4$ did not notably affect the structure of MgCl(OMe). Also IR and ^{13}C NMR spectroscopic data showed that the addition of $TiCl_4$ did not cause any major changes to the structure of MgCl(OMe), although magnesium alkoxides are known to be reactive towards $TiCl_4$. The result suggests that methoxy groups of MgCl(OMe) do not react with $TiCl_4$ under the reaction conditions used, although some changes in the local environment of $TiCl_4$ adsorption sites are possible. In accordance with our results, a recent combined experimental and computational study by D'Anna et al. showed a possible presence of EtO^- ligands on the surface of $MgCl_2$-$TiCl_4$ precatalyst with ethanol as an electron donor.[82]

Table 2. Chemical compositions (wt %) of MgCl(OMe), MgCl(OMe)-$TiCl_4$, MgCl(OMe)-DIBP, and MgCl(OMe)-EB complexes.

product	wt % (Mg)	wt % (Cl)[a]	wt % (OMe)	wt % (DMP)[b]	wt % (Ti)	wt % (DIBP)	wt % (EB)
MgCl(OMe)	24.5	44.9[c]	25.6	5.0	-	-	-
MgCl(OMe)-$TiCl_4$	23.9	45.1	24.6	4.3	2.1	-	-
MgCl(OMe)-DIBP	23.1	39.3	26.9	3.5	-	7.2	-
MgCl(OMe)-EB	24.6	37.1	26.5	3.6	-	-	8.2

[a]Cl content is based on calculations. [b]Unreacted 1,3-dimethoxypropane present in the products. [c]MgCl(OMe) contains some residual octane (solvent), leading to overestimation of Cl content.

IR spectroscopy is known to be a powerful tool for investigating complexes of carbonyl compounds, because the position of C=O stretching vibration is highly sensitive to coordination. The IR study of MgCl(OMe)-ester complexes indicated coordination of DIBP and EB to MgCl(OMe) through carbonyl group. C=O stretching bands of the complexes were deconvoluted using the Levenberg–Marquardt algorithm and the Gaussian line shape for a detailed analysis of ester electron donor coordination on MgCl(OMe) (**Figure 12**).

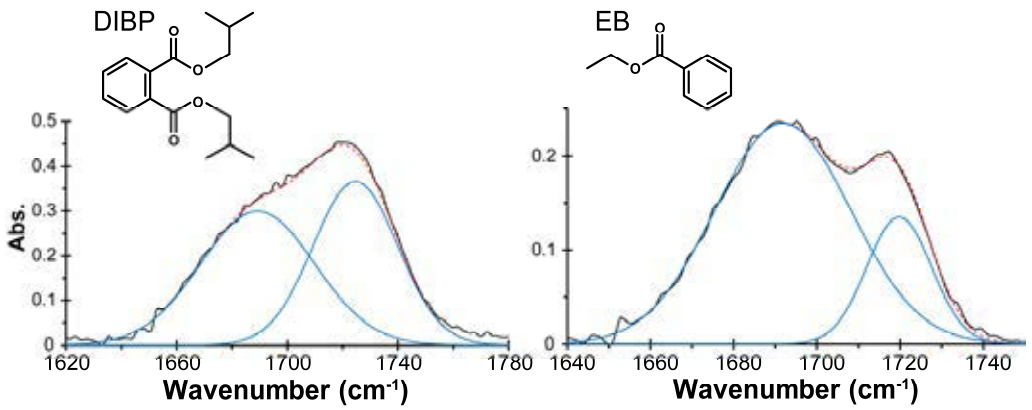

Figure 12. The deconvoluted carbonyl regions of IR spectra of MgCl(OMe)-DIBP (left) and MgCl(OMe)-EB (right) complexes, accompanied with structures of DIBP and EB. The black lines represent experimental spectra, the blue lines fitted individual peaks, and the red dashed lines the sums of the fitted peaks.

The C=O stretching band of MgCl(OMe)-DIBP complex is composed of two superimposed absorptions at 1725 and 1689 cm^{-1}. For unbound DIBP, the absorption of C=O stretching vibration is located at 1727 cm^{-1}, giving $\Delta\nu$(C=O) values of 2 and 38 cm^{-1} due to coordination to MgCl(OMe). For $MgCl_2$-DIBP-$TiCl_4$ system and $MgCl_2$-dibutyl phthalate complex, $\Delta\nu$(C=O) values as high as 72 and 78 cm^{-1}, respectively, have been reported.[15,43] The deconvolution of C=O stretching band suggests also in the case of MgCl(OMe)-EB complex the presence of two superimposed absorptions, which are located at 1719 and 1692 cm^{-1}. For free EB, the

corresponding absorption is located at 1719 cm^{-1}, giving $\Delta\nu$(C=O) values of 0 and 27 cm^{-1} due to coordination. For $MgCl_2$-EB-$TiCl_4$ system and $MgCl_2$-EB complex without $TiCl_4$, $\Delta\nu$(C=O) values as high as 69 cm^{-1} and 71 cm^{-1}, respectively, have been reported.[15,43] The significantly smaller C=O absorption shifts of MgCl(OMe)-electron donor complexes compared to those of the corresponding $MgCl_2$ complexes indicate notably weaker interaction of ester electron donors with MgCl(OMe) than with $MgCl_2$.

Coordination of $TiCl_4$ and ester electron donors on selected MgCl(OMe) and MgC_2 surfaces were studied by the means of periodic quantum chemical calculations. In order to make a practical comparison between the two support materials, the study focused on the catalytically relevant (104) and (110) surfaces of $MgCl_2$ and their analogous MgCl(OMe) counterparts, which are referred as (104)-like and (110)-like surfaces. In this study, the MgCl(OMe) surfaces were systematically cut in such a way that $MgCl_2$ and $Mg(OMe)_2$ surface units alternate in the periodic direction, although also other possibilities exist due to striped structure of MgCl(OMe) and the mixing of OMe and Cl units. Dimethyl phthalate was used as a model for DIBP in order to simplify the alkyl chain rotations. The optimized structures of the $TiCl_4$/donor coordinated MgCl(OMe) surfaces are presented in **Figure 13**. Energies of the corresponding surfaces are presented in **Table 3**, including a comparison to $MgCl_2$. The energies are reported with respect to a fully saturated crystalline layer and free adsorbates per surface length of an ångstrom in order to account for the relative stabilities of the donor coordinated surfaces and to enable comparison between different lateral surfaces.[55]

Table 3. Stabilities of the $TiCl_4$ and donor coordinated $MgCl_2$ and MgCl(OMe) surfaces.

	$MgCl_2$[a]		MgCl(OMe)[a]	
adsorbate	(104)	(110)	(104)-like	(110)-like
none	13.5	17.3	15.7	22.8
$TiCl_4$	–1.8	–2.5	–5.1	–7.7
dimethyl phthalate	–11.1	–13.9	–2.6	–3.1
ethyl benzoate	–20.7	–20.3	–6.8	–7.1

[a]The energies are given relative to the respective crystalline monolayer and free adsorbates in kJ/mol per a surface length of Å.

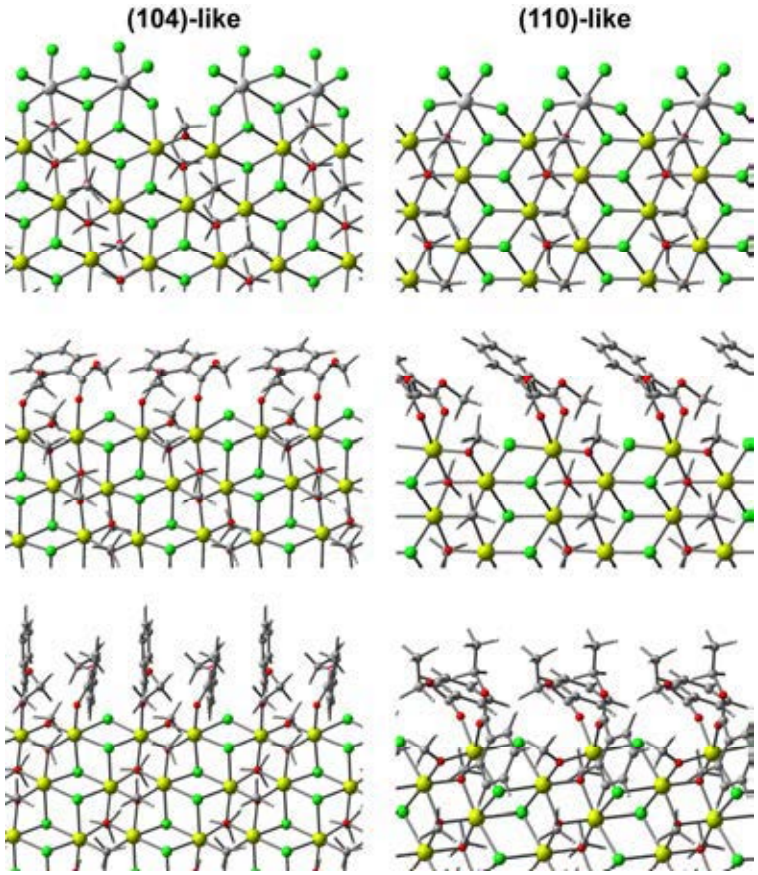

Figure 13. Coordination of $TiCl_4$ (top), dimethyl phthalate (middle) and ethyl benzoate (bottom) on the MgCl(OMe) (104)-like and (110)-like surfaces. Green = Cl, yellow = Mg, red = O, dark gray = C, light gray = Ti.

Computational results indicate that, as in the case of $MgCl_2$,[65] $TiCl_4$ on MgCl(OMe) prefers an octahedral 6-coordination on both of the studied surfaces. Hence, $TiCl_4$ prefers a binuclear binding on the (104)-like surface and a mononuclear binding on the (110)-like surface of MgCl(OMe). Dimethyl phthalate binds in a bridging mode on the (104)-like and in a chelate mode on the (110)-like surface of MgCl(OMe), whereas ethyl benzoate prefers coordination in a monodentate mode on the (104)-like surface and in a dual monodentate mode on the (110)-like surface of MgCl(OMe). Without $TiCl_4$/electron donors, the formation of the (104)-like and (110)-like surfaces of MgCl(OMe) is less favorable than the formation of the corresponding $MgCl_2$ surfaces. Coordination of $TiCl_4$ stabilizes MgCl(OMe) more than $MgCl_2$, whereas ester electron donors show an opposite effect, in accordance with the experimental results. $TiCl_4$ favors coordination on the (110)-like surface of MgCl(OMe), while no particular preference was found in the cases of studied electron donors.

3.1.4. Polymerization catalyst supported on MgCl(OMe)

Combined experimental and computational results indicated that the binding properties of MgCl(OMe) support differ notably from those of $MgCl_2$. On one hand, the stronger coordination of $TiCl_4$ on MgCl(OMe) with respect to $MgCl_2$ holds the potential for a high surface coverage of active titanium species and, thus, for a high activity in polymerization. On the other hand, the weaker coordination of ester electron donors on MgCl(OMe) with respect to $MgCl_2$ suggest that methoxymagnesium chloride could be a suitable support material for a catalyst in which an electron donor does not play a key role.

MgCl(OMe)-$TiCl_4$ precatalyst was examined in ethylene homopolymerization. Titanium content of MgCl(OMe)-supported catalyst was 2.1 wt %, which is a typical titanium content also in $MgCl_2$-supported precatalysts.[15,28] The relatively low titanium content of MgCl(OMe)-supported precatalyst can be explained by the presence of residual 1,3-dimethoxypropane in MgCl(OMe) support, blocking part of the possible coordination sites. The activity of MgCl(OMe)-$TiCl_4$ catalyst in ethylene polymerization was 470 $kg_{PE}/(mol_{Ti}h)$. For a comparison, the activity of $MgCl_2$-$TiCl_4$ catalyst (2.0 wt % Ti) prepared with the same method was only 190 $kg_{PE}/(mol_{Ti}h)$, giving almost 150% higher activity for MgCl(OMe)-supported catalyst. Overall, the experimental and computational results together indicate the potentiality of methoxymagnesium chloride as a support material for Ziegler–Natta type polymerization catalyst.

3.2. Crystalline magnesium chloride-electron donor complexes

Grignard–Wurtz synthesis in the presence of diether electron donors resulted in the cleavage reaction of diethers and the formation of methoxymagnesium chloride. Consequently, another synthetic procedure was needed to obtain magnesium chloride-diether complexes. The method involved recrystallization of δ-$MgCl_2$ in the presence of excess electron donor without using any additional solvent and resulted in the formation of crystalline complexes. The products were characterized using single-crystal X-ray crystallography and spectroscopic techniques. In addition to diethers, a diamine was studied as an electron donor in order to obtain a more comprehensive understanding of coordination of chelating donors to magnesium chlorides. The electron donors used in the study included 1,2-dimethoxyethane (DME), 1,3-dimethoxypropane (DMP) and *N*,*N*'-diethylethylenediamine (DEEDA) (structures **1**,**4**, and **5** in **Figure 4**).

3.2.1. Magnesium chloride-1,2-dimethoxyethane complex

Based on a single-crystal X-ray structure determination, the recrystallization of δ-$MgCl_2$ in the presence of 1,2-dimethoxyethane results in the formation of a polymeric complex $[MgCl_2(DME)]_n$ (**Figure 14**). The structure consists of a zig-zag type helical polymeric chain, in which adjacent Mg atoms are connected to each other with two bridging Cl ligands. In addition, every magnesium atom possesses one DME molecule in a chelate binding mode, making Mg centers 6-coordinated. Certain transition metal tetrahalides (e.g. $TcCl_4$, $ZrCl_4$, and $OsBr_4$) are known to possess similar edge-sharing octahedral chain structure.[134] Both the experimentally determined Mg/donor molar ratio (1.01) and PXRD data indicated homogeneity of the recrystallization product

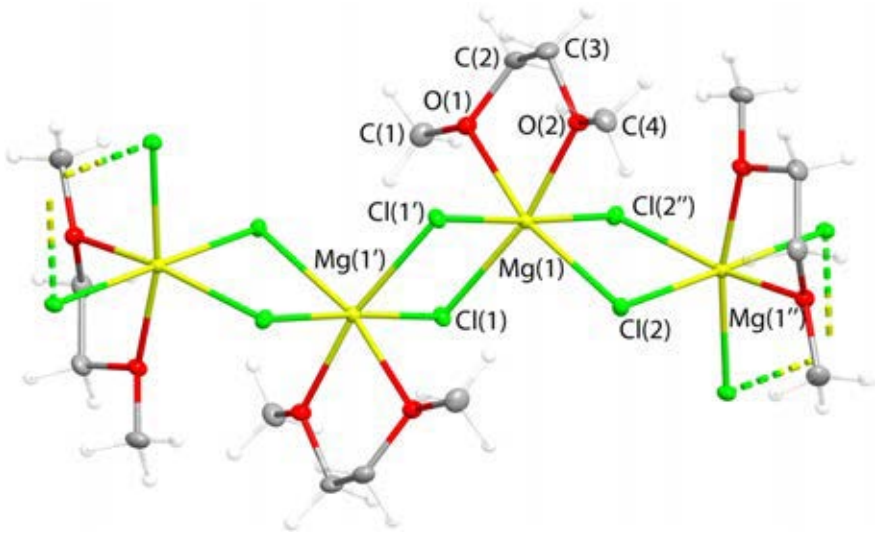

Figure 14. The crystal structure of the $[MgCl_2(DME)]_n$ complex. Thermal ellipsoids are shown at the 50% probability level. Green = Cl, yellow = Mg, red = O, gray = C.

The relatively short Mg–O bonds (2.13 and 2.17 Å) of the $[MgCl_2(DME)]_n$ complex together with a short distance between coordinated oxygen atoms of DME result in the formation of a 5-membered chelate ring possessing a small O–Mg–O bond angle of 74.9°. Consequently, the Mg atoms of the $[MgCl_2(DME)]_n$ complex possess a distorted octahedral coordination geometry. The formation of the stable $[MgCl_2(DME)]_n$ complex, despite the apparent ring strain, suggests a strong coordination ability of 1,2-diethers on $MgCl_2$.

The $[MgCl_2(DME)]_n$ complex can be considered as a structural model for the layered $MgCl_2$, providing further insight into possible Mg coordination sites. There is a clear congruence between the local coordination geometries of Mg atoms in the $[MgCl_2(DME)]_n$ complex and Mg atoms of the $MgCl_2$ (110) surface with coordinated diether molecules. However, it must be noted that the steric environment of these two coordination sites are different, as the adjacent coordination sites on the (110) surface of $MgCl_2$ point into same direction and on the $[MgCl_2(DME)]_n$ complex are arranged helically around the $MgCl_2$ backbone chain. The crystal structure of the polymeric $[MgCl_2(DME)]_n$ complex provides further support for the preferential coordination of diethers on the (110) surface of $MgCl_2$ in a chelate binding mode.

The $[MgCl_2(DME)]_n$ complex differs notably from another magnesium chloride-1,2-dimethoxyethane complex with the formula $[MgCl_2(DME)_2]$ earlier reported by Neumüller et al.[100] $[MgCl_2(DME)]_n$ has a polymeric chain structure, while the crystal structure of the $[MgCl_2(DME)_2]$ molecular complex is composed of individual $[MgCl_2(DME)_2]$ molecules packed in a lattice. The structures of several polymeric magnesium chloride complexes containing e.g. ethanol, THF, and esters as electron donors, have been published.[76,77,89,94,95] However, none of reported complexes contain chelating electron donors. The crystal structure of the $[MgCl_2(DME)]_n$ complex unambiguously shows that polymeric magnesium chloride-electron donor species can be formed also in the case of industrially important diether electron donors.

The CP/MAS ^{13}C NMR spectrum of the $[MgCl_2(DME)]_n$ complex (**Figure 15**) shows two distinct carbon resonances for CH_2 groups (C2 and C3), located at 71.4 and 70.7 ppm. The corresponding signal for unbound DME is located at 71.8 ppm, indicating minor upfield shifts due to coordination. The appearance of two CH_2 carbon resonances can be rationalized by the solid-state structure of the complex, in which the two ether groups were found to be crystallographically nonequivalent with different local environments and Mg–O bond lengths (2.13 and 2.17 Å). An IR study (**Figure 16**) provided further support for the different local environments of ether groups in the $[MgCl_2(DME)]_n$ complex, as the asymmetric C–O–C stretching vibration of free DME at approximately 1110 cm^{-1} is replaced with multiple absorptions bands at lower wavenumbers in the IR spectrum of the $[MgCl_2(DME)]_n$ complex.

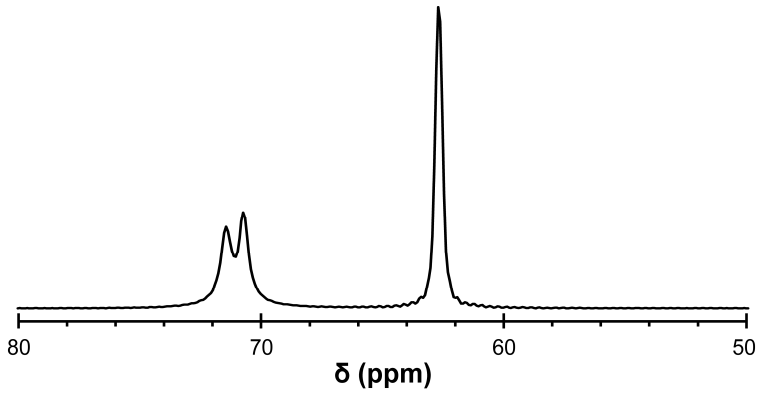

Figure 15. CP/MAS ^{13}C NMR spectrum of the $[MgCl_2(DME)]_n$ complex.

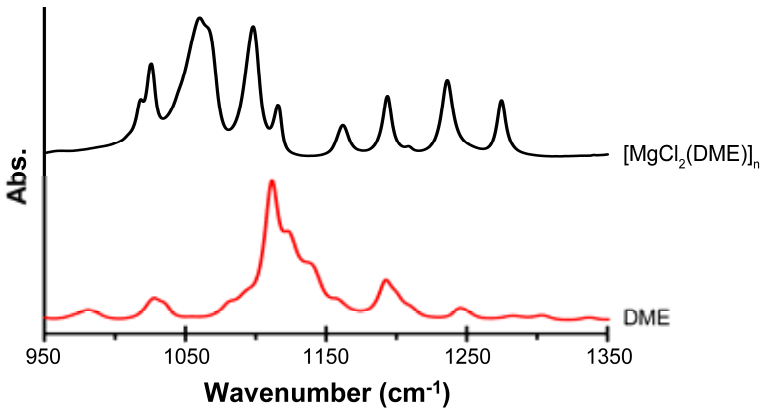

Figure 16. IR spectra (region 950–1350 cm^{-1}) of DME in a solution of CCl_4 (red line) and the $[MgCl_2(DME)]_n$ complex (black line).

3.2.2. Magnesium chloride-1,3-dimethoxypropane complex

The crystal structure of $[Mg_2Cl_4(DMP)_2(H_2O)]$ complex formed in the reaction between δ-$MgCl_2$ and 1,3-dimethoxypropane is presented in **Figure 17**. The X-ray structure determination revealed two different types of Mg atoms. One of the Mg atoms has a tetrahedral coordination with four Cl ligands, one of which is bridging between the two types of Mg atoms. In addition to the μ_2-

bridging Cl ligand, the other Mg atom possesses two DMP molecules in a chelate binding mode and a water molecule, making it 6-coordinated. The longer O–O distance of DMP compared to that of DME results in the formation of 6-membered chelate rings having more favorable O–Mg–O bond angles of 86.6° and 86.3°. Thus, the 6-coordinated Mg atom of the $[Mg_2Cl_4(DMP)_2(H_2O)]$ complex is able to adopt a nearly ideal octahedral coordination geometry. Both the PXRD data and Mg/donor ratio (1.18) indicated a presence of a minor amount of other compounds in the recrystallization product.

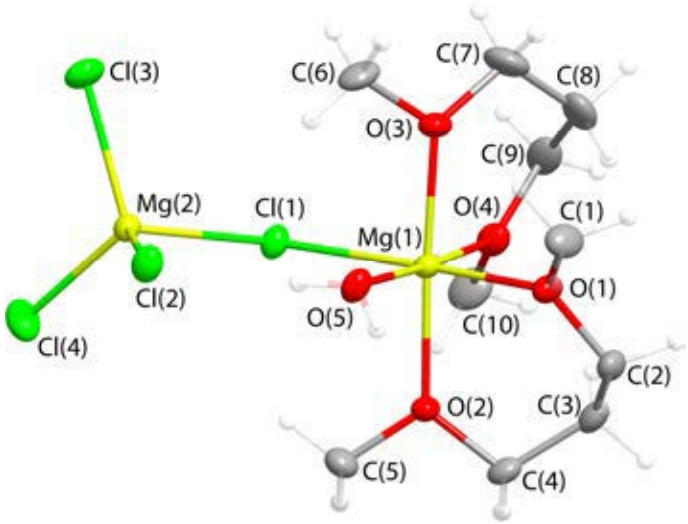

Figure 17. The crystal structure of the $[Mg_2Cl_4(DMP)_2(H_2O)]$ complex. Thermal ellipsoids are shown at the 50% probability level. Green = Cl, yellow = Mg, red = O, gray = C.

Each unit cell contains four $[Mg_2Cl_4(DMP)_2(H_2O)]$ complexes. A ^1H NMR study revealed the presence of residual water in 1,3-dimethoxypropane donor despite extensive drying, giving a reasonable explanation for the origin of the water molecule in the $[Mg_2Cl_4(DMP)_2(H_2O)]$ complex. Both intramolecular and intermolecular hydrogen bonding between the hydrogen atoms of the water molecule and chloride anions were found to be present, hence stabilizing the complex and the crystal form. Other magnesium chloride-electron donor complexes with water molecules in their structures have been previously reported.[91,96]

The CP/MAS ^{13}C NMR spectrum of the $[Mg_2Cl_4(DMP)_2(H_2O)]$ complex (**Figure 18**; left) exhibits multiple overlapping resonances for α-CH_2 (C2, C4, C7, C9) and α-CH_3 (C1, C5, 67, C10) groups of 1,3-dimethoxypropane molecules. In order to make a detailed analysis, the region of α-carbon resonances (58–76 ppm) was deconvoluted using the Levenberg–Marquardt algorithm and the Lorentzian line shape (**Figure 18**; right). The deconvolution suggests that both α-carbon signals are composed of four distinct peaks with approximately equal integrals. All the fitted peaks are shifted downfield with respect to corresponding resonances of free DMP. The appearance of multiple α-carbon peaks indicates a nonequivalency of the four ether groups in the complex, which is in agreement with the structural data.

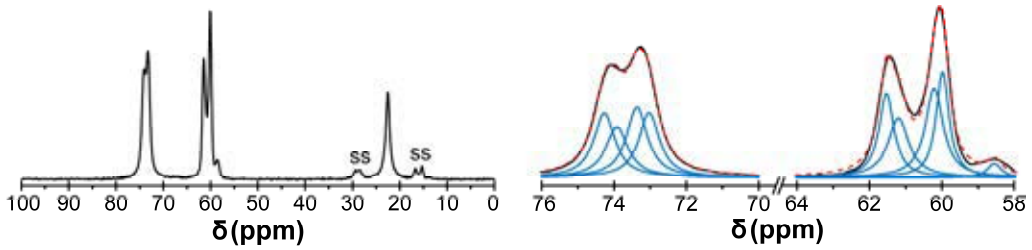

Figure 18. CP/MAS ^{13}C NMR spectrum of the $[Mg_2Cl_4(DMP)_2(H_2O)]$ complex (left) and the deconvolution of α-carbon region (right). The black line represents experimental spectrum, the blue lines fitted individual peaks, and the red dashed line the sum of the fitted peaks. ss = spinning sideband of α-CH_3 and α-CH_2 groups.

The IR spectrum of the $[Mg_2Cl_4(DMP)_2(H_2O)]$ complex is presented in **Figure 19**. The asymmetric C–O–C stretching vibration of free DMP located approximately at 1120 cm^{-1} is replaced with multiple absorptions at lower wavenumbers in the IR spectrum of the $[Mg_2Cl_4(DMP)_2(H_2O)]$ complex. The IR result indicates nonequivalent positions of ether groups in the complex, consistent with the XRD and ^{13}C NMR data. In addition, the IR spectrum of the $[Mg_2Cl_4(DMP)_2(H_2O)]$ complex exhibits absorptions at 1620, 3455, and 3500 cm^{-1}, which are probably due to water molecule present in the structure.

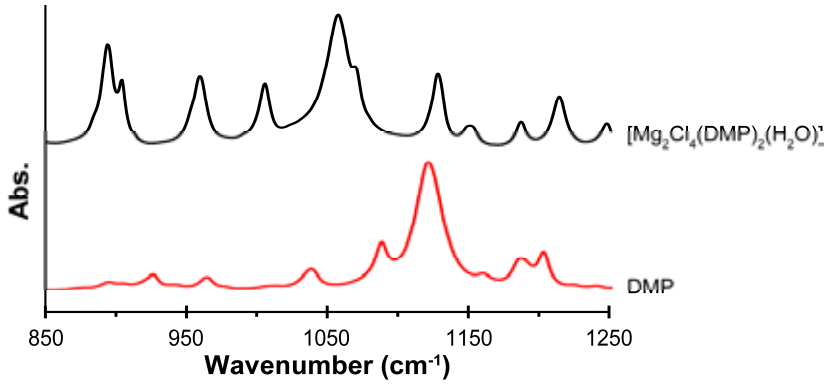

Figure 19. IR spectra (region 850–1250 cm^{-1}) of DMP in a solution of CCl_4 (red line) and the $[Mg_2Cl_4(DMP)_2(H_2O)]$ complex (black line).

3.2.3. Magnesium chloride-*N,N'*-diethylethylenediamine complex

The recrystallization of δ-$MgCl_2$ in the presence of *N,N'*-diethylethylenediamine results in the formation of a centrosymmetric complex with a molecular formula $[MgCl_2(DEEDA)_2]$ (**Figure 20**). The structure consists of 6-coordinated Mg atoms having two Cl ligands *trans* to each other and two DEEDA molecules in a chelate binding mode. The longer Mg–N and C–N bond lengths of the $[MgCl_2(DEEDA)_2]$ complex with respect to the Mg–O and C–O bond lengths of the $[MgCl_2(DME)]_n$ complex result in the formation of less strained 5-membered chelate rings. Hence, the coordination geometry of Mg centers deviates only somewhat from an ideal octahedral coordination geometry (N–Mg–N bond angle of 81.4°). The experimentally determined

Mg/donor molar ratio (0.52) and PXRD data indicated homogeneity of the recrystallization product.

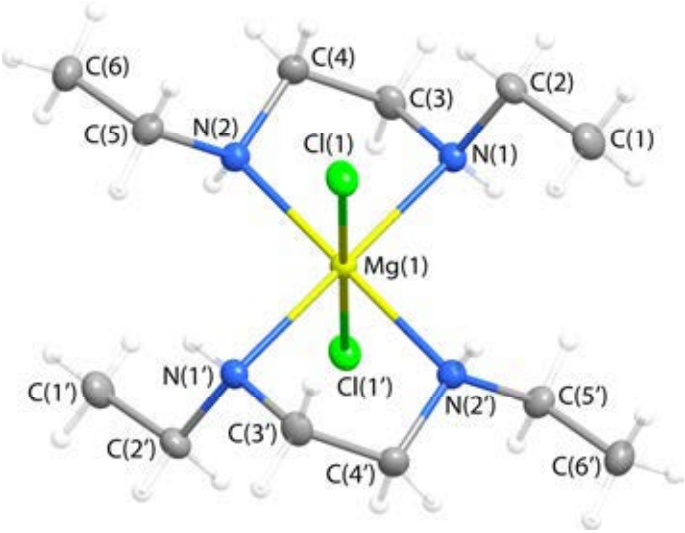

Figure 20. The crystal structure of the $[MgCl_2(DEEDA)_2]$ complex. Thermal ellipsoids are shown at the 50% probability level. Green = Cl, yellow = Mg, blue = N, gray = C.

As in the case of the $[Mg_2Cl_4(DMP)_2(H_2O)]$ complex, the CP/MAS ^{13}C NMR spectrum of the $[MgCl_2(DEEDA)_2]$ complex presented in **Figure 21** exhibits multiple partly overlapping α-carbon (CH_2 groups directly connected to N) resonances. The deconvolution suggests the α-carbon region consists of three distinct peaks at 51.3, 46.2, and 44.9 ppm. The appearance of multiple CH_2 resonances indicates, in agreement with the structural data, nonequivalent positions of amino groups in the complex. In addition, the CP/MAS ^{13}C NMR spectrum of the $[MgCl_2(DEEDA)_2]$ complex exhibits two distinct resonances (16.3 and 14.5 ppm) also for the crystallographically nonequivalent CH_3 groups (C1 and C6).

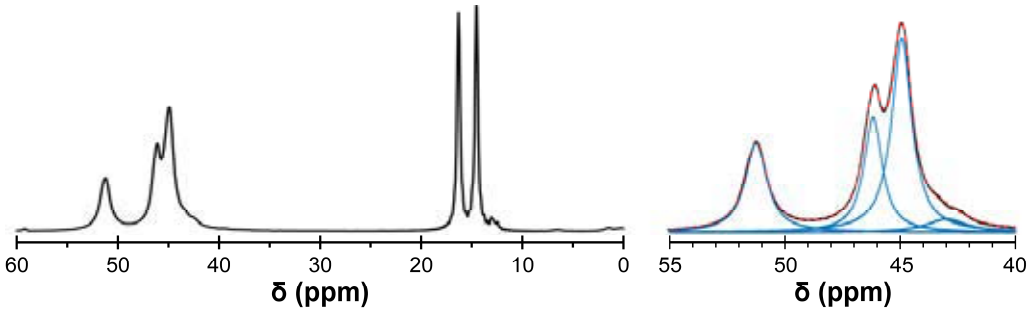

Figure 21. CP/MAS ^{13}C NMR spectrum of the $[MgCl_2(DEEDA)_2]$ complex (left) and the deconvolution of α-carbon region (right). The black line represents experimental spectrum, the blue lines fitted individual peaks, and the red dashed line the sum of the fitted peaks.

The IR spectrum of the [$MgCl_2(DEEDA)_2$] complex (**Figure 22**) exhibits multiple sharp absorptions in the region typical for C–N stretching vibration (1000–1200 cm^{-1}). Some of the absorptions have been shifted towards lower wavenumbers with respect to free DEEDA (1120 cm^{-1}). Furthermore, the broad N–H stretching absorption (3280 cm^{-1}) and C–H stretching absorption of NCH_2 group (2820 cm^{-1}) of free DEEDA have been replaced with multiple sharp absorptions due to coordination. Overall, the IR results are in agreement with the XRD and NMR data, indicating coordination of DEEDA through N atoms to magnesium and nonequivalent positions of amino groups in the complex.

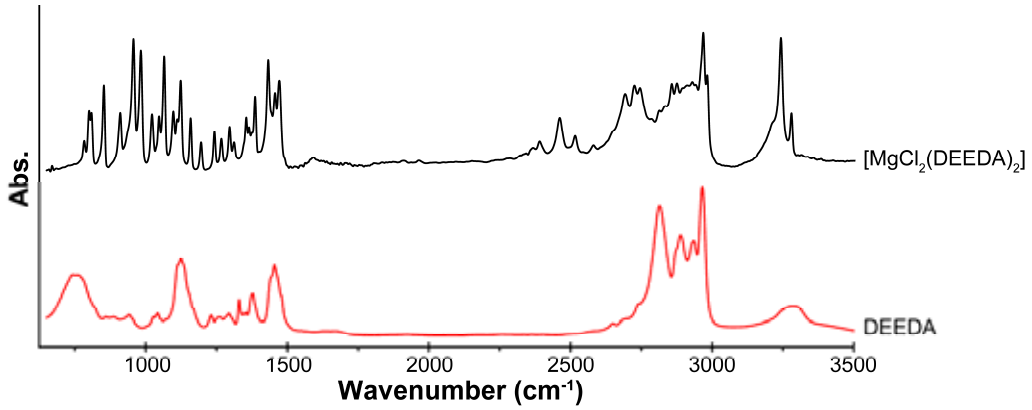

Figure 22. IR spectra of free DEEDA (red line) and the [$MgCl_2(DEEDA)_2$] complex (black line).

3.3. Polyethylenimines as electron donors for Ziegler–Natta catalysts

Inspired by the formation of the crystalline [$MgCl_2(DEEDA)_2$] complex, polyethylenimines (PEIs), polymers bearing amino functionalities, were studied as new possible multidentate electron donors for Ziegler–Natta catalysts. A major advantage of PEIs in comparison to the conventional electron donors (e.g. phthalates) is their relative harmlessness. As a matter of fact, PEI is frequently studied in biochemical and pharmaceutical applications, particularly in a gene/drug delivery.[135,136] A commercially available, relatively low molar mass (M_w = 800 g/mol) branched polyethylenimine was used in the study. The structure of branched PEI, containing various primary, secondary, and tertiary amino groups, is presented in **Figure 4** (structure **6**).

3.3.1. Interaction of PEI with $MgCl_2$

Interaction of PEI with $MgCl_2$ support was studied by adding branched PEI to δ-$MgCl_2$, which had been prepared using Grignard–Wurtz coupling reactions. A Mg/donor molar ratio was varied in order to obtain complexes with varying composition (**Table 4**). In the cases of molar ratios of 1:0.5 and 1:1, most of the polyethylenimine added to the reaction mixtures was also present in the products, indicating a strong coordination ability of branched PEI. Increasing the amount of PEI in the reaction mixture further (molar ratio of 1:5) did not result in a product with a considerably higher PEI content, indicating saturation of $MgCl_2$ surface with PEI. Based on PXRD results (**Figure 23**), the addition of branched PEI to $MgCl_2$ did not affect significantly the

structure of δ-$MgCl_2$, as all the prepared $MgCl_2$-PEI complexes were highly disordered, showing the typical characteristics of δ-$MgCl_2$.

Table 4. Chemical compositions of $MgCl_2$-PEI complexes.

reaction mixture	product		
n(Mg):n(PEI)[a]	n(Mg):n(PEI)[a]	wt % (Mg)	wt % (PEI)
1:0.5	1:0.47	19.6	16.4
1:1	1:0.85	15.5	23.2
1:5	1:1.23	12.9	28.2

[a]Mg/PEI molar ratios are given relative to repeating units of PEI (CH_2–CH_2–NH).

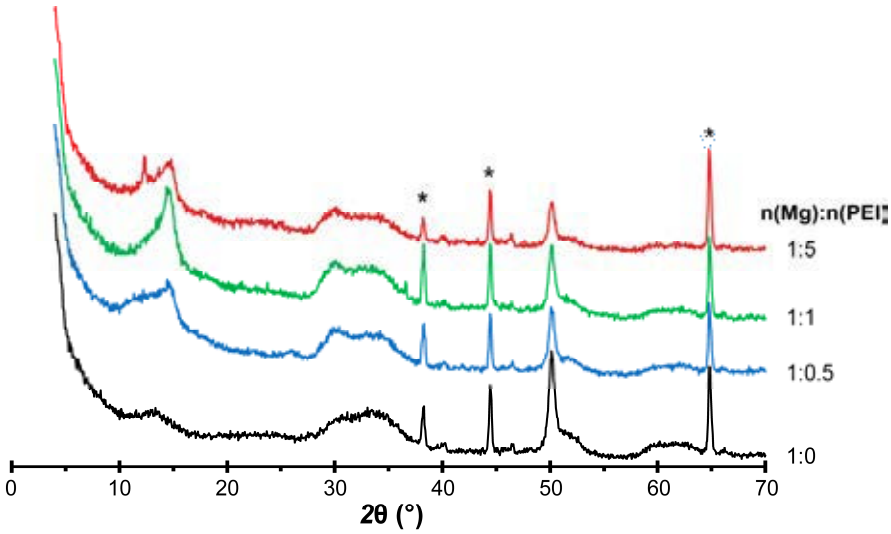

Figure 23. Powder X-Ray diffraction patterns of $MgCl_2$-PEI complexes. Reference product n(Mg):n(PEI) = 1:0 refers to δ-$MgCl_2$, which was heated in toluene in the absence of an electron donor. Reflections of the sample holder are marked with asterisks (*).

The branched structure of PEI enables its coordination to $MgCl_2$ through different amino groups. Based on ^{13}C NMR results (**Figure 25**), the polyethylenimine used in this study contains primary, secondary, and tertiary amino groups approximately in a molar ratio of 1.8:1.5:1, respectively. The IR spectra of $MgCl_2$-PEI complexes are presented in **Figure 24**. The C–N stretching vibrations of $MgCl_2$-PEI complexes (870–1180 cm^{-1}) have shifted towards lower wavenumbers with respect to unbound PEI (1000–1200 cm^{-1}), indicating coordination of PEI through nitrogen atoms on $MgCl_2$ surface. Furthermore, the shifting and broadening of the C–N stretching bands suggest that N atoms of all types of amino groups (primary, secondary, and tertiary) can coordinate to unsaturated Mg atoms. The CP/MAS ^{13}C NMR spectrum of $MgCl_2$-PEI complex (**Figure 25**) shows at least three partly overlapping signals in the region 35–65 ppm. The broadening of all resonances indicates multiple possible chemical environments of primary,

secondary, and tertiary amino groups in $MgCl_2$-PEI complexes. Thus, the NMR data suggests, in accordance with the IR results, coordination of PEI to $MgCl_2$ using all the three types of amino groups.

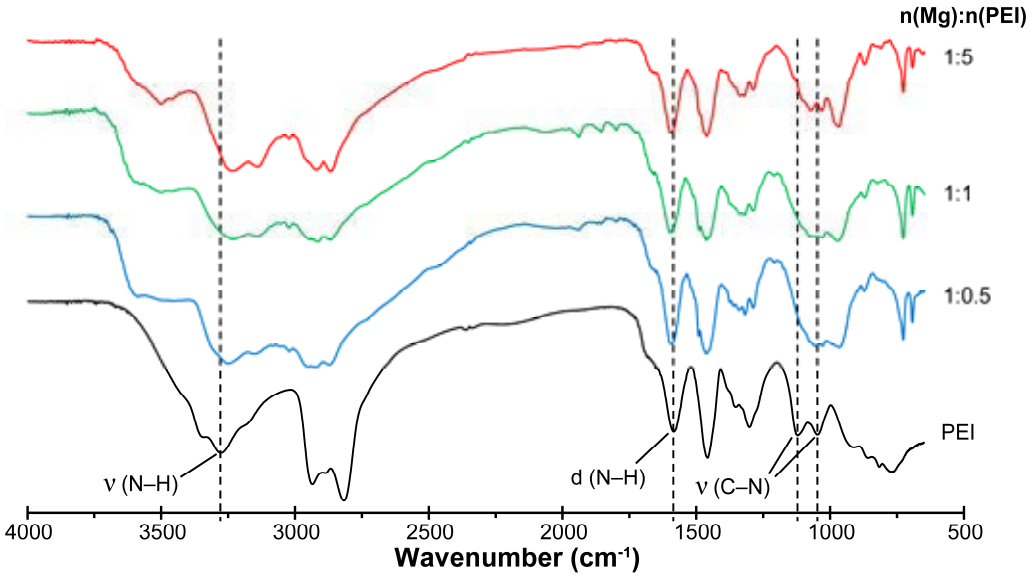

Figure 24. IR spectra of unbound PEI and $MgCl_2$-PEI complexes.

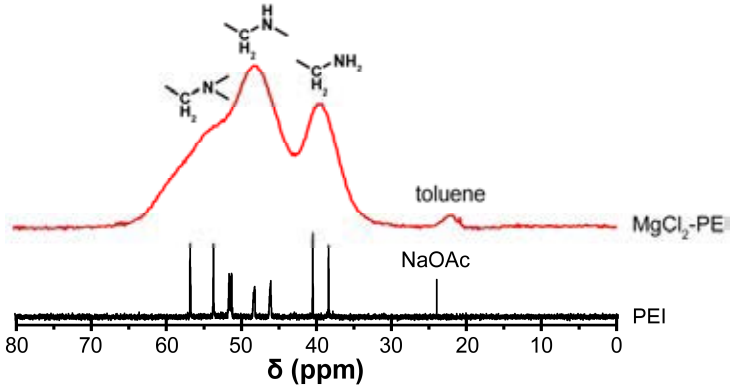

Figure 25. ^{13}C NMR spectra of unbound PEI (in a solution of D_2O) and $MgCl_2$-PEI complex (solid state) (n(Mg):n(PEI) = 1:5). In the case of unbound PEI, sodium acetate (NaOAc) was used as an internal standard.

The structural and energetic features of $MgCl_2$-PEI complexes were further investigated using a computational approach. Coordination of linear and branched polyethylenimines on the catalytically relevant (104) and (110) surfaces of $MgCl_2$ were studied by the means of periodic calculations. Several different models of polyethylenimine (**Figure 26**) were employed in the calculations to simultaneously account for the effect of branching and stereochemical configuration of PEI (isotactic and syndiotactic forms). In addition, dimethyl phthalate was also included in the study to enable a comparison of the $MgCl_2$ surface stabilization by polyethylenimines to the surface stabilization by the conventional bidentate electron donor. The optimized structures of PEIs coordinated on the (104) and (110) surfaces are presented in **Figure 27** and the corresponding stabilization energies of the electron donor coordinated surfaces in **Table 5**. As in the case of calculations concerning the interaction of electron donors with MgCl(OMe) support, the energies are reported with respect to a fully saturated $MgCl_2$ layer and free adsorbates per a length of surface (Å) in the periodic direction.[55]

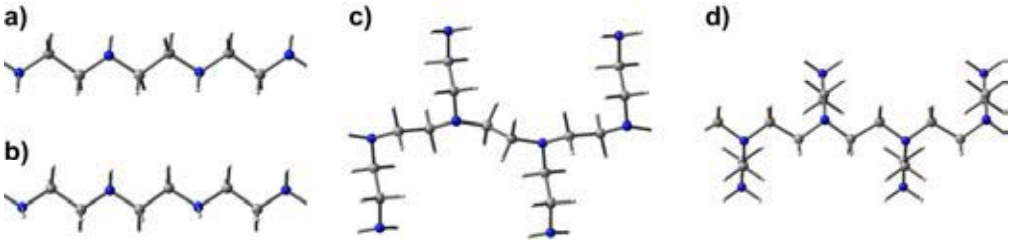

Figure 26. Fragments of infinitely long a) isotactic linear PEI, b) syndiotactic linear PEI, c) isotactic branched PEI, and d) syndiotactic branched PEI models employed in the periodic calculations. Blue = N, gray = C.

Table 5. Stabilities of the electron donor coordinated $MgCl_2$ surfaces.

electron donor	(104)[a]	(110)[a]
dimethyl phthalate	–11.1	–13.9
isotactic linear PEI	–5.8	–9.0
syndiotactic linear PEI	–10.5	–17.9
isotactic branched PEI	–15.2	–27.9
syndiotactic branched PEI	–16.1	–33.8

[a]The energies are given relative to crystalline monolayer and free electron donors in kJ/mol per a surface length of Å.

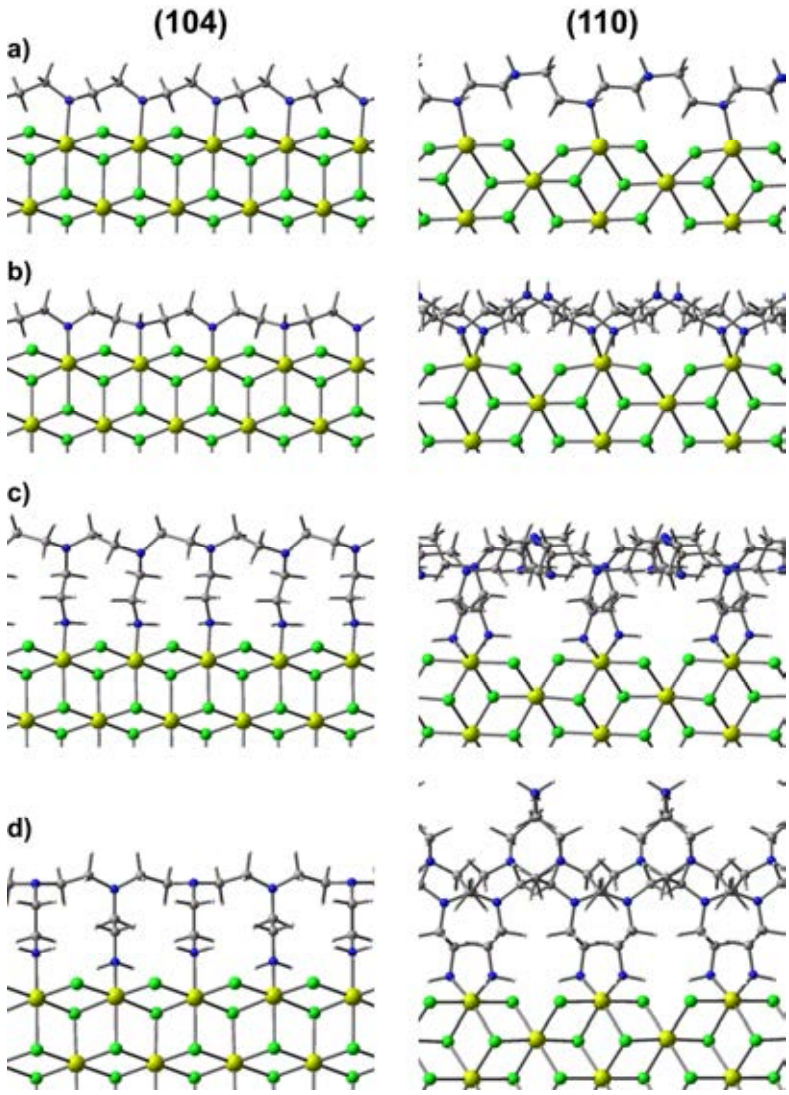

Figure 27. Coordination of a) isotactic linear PEI, b) syndiotactic linear PEI, c) isotactic branched PEI, and d) syndiotactic branched PEI on the $MgCl_2$ (104) and (110) surfaces. Green = Cl, yellow = Mg, blue = N, gray = C.

The theoretical results obtained suggest that the structural variations significantly affect the ability of PEI to stabilize the lateral surfaces of $MgCl_2$. The isotactic form of linear PEI possesses surface stabilization energies somewhat lower than those of dimethyl phthalate. Lower surface stabilization energies are due to poor matching of polymer N–N distances and surface Mg–Mg distances. In addition, the short distance between polymer backbone chain and $MgCl_2$ surface results in strong repulsion further destabilizing the surface. The stabilization energies increase from the (104) to the (110) surface due to longer Mg–Mg separation of the (110) surface, which offers a greater fluxionality and, thus, reduced strain. The matching of polymer N–N distances and surface Mg–Mg distances is better for syndiotactic linear PEI and the chain configuration of syndiotactic linear PEI allows simultaneous coordination of two polymer chains on the (110)

surface, making surface Mg atoms 6-coordinated. The resulting relatively high stabilization energy of –17.9 kJ/mol/Å suggests that the intermolecular dispersive interactions play an important role in the surface stabilization.

Coordination of branched PEIs stabilizes the (104) and (110) surfaces of $MgCl_2$ significantly more than either dimethyl phthalate or linear PEIs. The higher stabilization energies are most probably due to higher flexibility of branched structure and larger separations between polymer backbone chains and $MgCl_2$ surfaces, resulting in reduced repulsion. Intramolecular and intermolecular dispersive interaction on the (104) and (110) surfaces, respectively, further stabilize the surfaces. Intermolecular interactions of polymeric chains on the (110) surface are stronger, and especially strong in the case of syndiotactic branched PEI, resulting in a high stabilization energy of –33.8 kJ/mol/Å.

3.3.2. Polymerization catalyst with PEI as internal electron donor

In order to evaluate the effect of branched PEI as internal electron donor on the polymerization performance of an industrially relevant $MgCl_2$-supported Ziegler–Natta catalyst, a $MgCl_2$-PEI-$TiCl_4$ precatalyst was prepared by a sequential addition of low molar mass branched PEI and $TiCl_4$ to a $MgCl_2$-EtOH adduct[116–118]. A precatalyst containing 24.4 wt % of PEI, 12.6 wt % of Mg, 4.2 wt % of Ti, and 1.5 wt % of EtO was obtained. The high amount of PEI present in the product indicates that even extensive washing cannot remove PEI from the precatalyst. The spectroscopic data indicated coordination of PEI through nitrogen atoms to $MgCl_2$ also in the case of $MgCl_2$-PEI-$TiCl_4$ precatalyst.

The $MgCl_2$-PEI-$TiCl_4$ catalyst performed well in the copolymerization of ethylene and 1-butene. The activity of the $MgCl_2$-PEI-$TiCl_4$ catalyst (9.5 $kg_{polymer}/(g_{cat}h)$) was 40 % higher than that of a $MgCl_2$-supported reference catalyst containing bis(2-ethylhexyl) phthalate as an internal electron donor (6.7 $kg_{polymer}/(g_{cat}h)$)[137]. However, the $MgCl_2$-PEI-$TiCl_4$ catalyst exhibited somewhat lower comonomer response than the phthalate-containing reference catalyst[137]. In conclusion, the polymerization results indicate the potential of branched polyethylenimine as an internal electron donor for Ziegler–Natta type polymerization catalysts.

4. Conclusions

The structure of magnesium chloride support and the coordination of electron donors are known to be important factors for the performance of Ziegler–Natta catalysts. The use of suitable electron donors is essential for obtaining a catalyst with desired properties. Conventionally electron donors are assumed to coordinate on the lateral surfaces of $MgCl_2$ and, hence, affect the structure of support material and properties of active polymerization sites. However, in the case of certain electron donors also crystalline magnesium chloride-electron donor complexes can be formed. In this study, the effect of industrially important diether electron donors on the crystal structures of magnesium chlorides was investigated. Also multidentate amine electron donors were included in the study to generalize the results for nitrogen-containing electron donors.

When a simple diether, 1,3-dimethoxypropane, was used as an electron donor in Grignard–Wurtz synthesis of a $MgCl_2$-electron donor complex, it was unexpectedly observed to undergo a cleavage reaction, resulting in the formation of methoxymagnesium chloride. Diether acts as a source of methoxy groups. The solid reaction product (MgCl(OMe)), was found to possess a layer structure similar to that of $MgCl_2$. Combined experimental and theoretical results highlight the potential of MgCl(OMe) as a support material for a Ziegler–Natta type polymerization catalyst, in which electron donors do not play a key role. On the other hand, the possible cleavage of diethers can be adverse and must thus be taken into account when preparing Ziegler–Natta catalysts with diether electron donors.

Recrystallization of δ-$MgCl_2$ in the presence of chelating electron donors resulted in the formation of crystalline magnesium chloride-electron donor complexes. In the case of 1,2-dimethoxyethane, the recrystallization product was a polymeric complex $[MgCl_2(DME)]_n$, which can be considered as a structural model for the building unit of layered $MgCl_2$. In the cases of 1,3-dimethoxypropane and *N*,*N*'-diethylethylenediamine, recrystallizations resulted in the formation of $[Mg_2Cl_4(DMP)_2(H_2O)]$ and $[MgCl_2(DEEDA)_2]$ complexes. The results obtained clearly show, how diether and diamine electron donors can dictate the crystal structure of $MgCl_2$, not only by coordinating on the lateral surfaces, but also by forming crystalline complexes.

Polyethylenimines were studied for the first time as electron donors for Ziegler–Natta catalysts. Experimental and computational results together indicate a strong coordination ability of branched PEI on $MgCl_2$ surfaces through N atoms. According to quantum chemical calculations, the structural variations in PEI notably affect its ability to stabilize the lateral surfaces of $MgCl_2$, suggesting that the binding properties of polyethylenimines can be tailored through structural modifications. The $MgCl_2$-PEI-$TiCl_4$ catalyst showed a relatively high activity in ethylene/1-butene copolymerization, highlighting the potential of polyethylenimines as alternatives for conventional electron donors.

In conclusion, the study revealed interesting aspects of the roles of multidentate ether and amine electron donors in the crystal structure formation of magnesium chlorides. The electron donors can react to other compounds during support preparation, form a crystalline magnesium chloride-electron donor complex or coordinate on the lateral surfaces of $MgCl_2$. The role, which an electron donor takes in the crystal structure formation, is highly dependent on the functionality of the electron donor, as well as on the synthesis method and reaction conditions utilized. The

simple diethers and diamine used in the study seem to favor the formation of crystalline magnesium chloride-electron donor complexes, if able to withstand the reaction conditions. In the case of a polymeric amine electron donor (PEI), the formation of $MgCl_2$-donor surface complex seems to be preferred. Surface complex formation has been reported to take place also in the case of substituted 1,3-diethers.[69] The results suggest that, in addition to functionality, also other structural factors of an electron donor can play a key role in the crystal structure formation of magnesium chlorides. The different behavior of electron donors can have important implications from the catalyst point of view and must thus be considered when preparing or modelling Ziegler–Natta catalysts.

Acknowledgements

The work was carried out at the Department of Chemistry, University of Eastern Finland during the years 2013–2017. Financial support from Polymer Research Initiative project funded by the Finnish Funding Agency for Technology and Innovation, as well as from Sirius Models and Experiment 2014–2016 project funded by Borealis Polymers Oy is gratefully acknowledged. Furthermore, a scholarship to the author from University of Eastern Finland is acknowledged.

I am deeply grateful to my supervisor Professor Tuula Pakkanen for believing in me and for offering me the possibility to work in the field of Ziegler–Natta catalysis. Thank you for sharing your knowledge with me and guiding me throughout my scientific career.

During the course of my work, I have had the pleasure to work with many fantastic people. I am especially grateful to Professors Mikko Linnolahti, Igor Koshevoy, and Tapani Pakkanen as well as to Doctors Sami Pirinen and Andrey Bazhenov for valuable discussions and cooperation. I also want to thank Dr. Peter Denifl, MSc Timo Leinonen, Dr. Anneli Pakkanen and Dr. Kumudini Jayaratne from Borealis Polymers Oy for introducing me to the world of industrial catalysis. I deeply appreciate all the advice and positive feedback I got during our fruitful cooperation. It has been an honor to work with such skillful scientists.

All the colleagues and personnel at the Department of Chemistry are thanked for generating a pleasant and inspiring working environment. I am deeply grateful to my two office mates Dr. Janne Salstela and MSc Hanna Paananen. Your support and encouragement have been extremely important. You were always there for me, when a second opinion or second pair of hands were needed. A special thanks goes also to Päivi Inkinen for all the practical help in the laboratory.

I want to thank all my friends for bringing joy and other interesting things, besides chemistry, to my life. My warmest thanks goes to my parents Juhani and Kirsti and to my brother Tuomo. You have always encouraged me to pursue my dreams. I cannot express, how much your love and support have meant to me. Last but not least, my loving thanks goes to my girlfriend Camilla. Our life together has not been the easiest, but still you have always been there for me. Thank you.

Joensuu, June 2017 *Ville Nissinen*

References

[1] Baker, A.-M. M.; Mead, J. In *Handbook of Plastics, Elastomers & Composites*, 4th ed.; Harper, C. A., Ed.; McGraw-Hill: USA, 2002; pp. 1–2.

[2] Kashiwa, N. The Discovery and Progress of $MgCl_2$-Supported $TiCl_4$ Catalysts. *J. Polym. Sci., Part A: Polym. Chem.* **2004**, *42*, 1–8.

[3] Pasquini, N.; Moore, E. P., Jr. In *Polypropylene Handbook*, 2nd ed.; Pasquini, N., Ed.; Hanser: Munich, 2005; pp. 6–12.

[4] Böhm, L. L. Ethylene Polymerization with Ziegler Catalysts: Fifty Years after the Discovery. *Angew. Chem., Int. Ed.* **2003**, *42*, 5010–5030.

[5] Albizzati, E.; Cecchin, G.; Chadwick, J. C.; Collina, G.; Giannini, U.; Morini, G.; Noristi, L. In *Polypropylene Handbook*, 2nd ed.; Pasquini, N., Ed.; Hanser: Munich, 2005; pp. 15–64.

[6] Chadwick, J. C.; Garoff, T.; Severn, J. R. In *Tailor-Made Polymers: Via Immobilization of Alpha-Olefin Polymerization Catalysts*; Severn, J. R., Chadwick, J. C., Eds.; WILEY-VCH: Weinheim, 2008; pp. 43–56.

[7] Liu, B.; Nitta, T.; Nakatani, H.; Terano, M. Specific Roles of Al-Alkyl Cocatalyst in the Origin of Isospecificity of Active Sites on Donor-Free $TiCl_4/MgCl_2$ Ziegler–Natta Catalyst. *Macromol. Chem. Phys.* **2002**, *203*, 2412–2421.

[8] Kissin, Y. V.; Liu, X.; Pollick, D. J.; Brungard, N. L.; Chang, M. Ziegler–Natta Catalysts for Propylene Polymerization: Chemistry of Reactions Leading to the Formation of Active Centers. *J. Mol. Catal. A: Chem.* **2008**, *287*, 45–52.

[9] Busico, V.; Cipullo, R.; Mingione, A.; Rongo, L. Accelerating the Research Approach to Ziegler–Natta catalysts. *Ind. Eng. Chem. Res.* **2016**, *55*, 2686–2695.

[10] Halden, R. U. Plastics and Health Risks. *Annu. Rev. Public Health* **2010**, *31*, 179–194.

[11] Ali, S. Polyolefin Catalyst Market Overview. *Catal. Rev.* **2014**, *27*, 7–14.

[12] Bosowska, K.; Nowakowska, M. The Roles for a Lewis Base and $MgCl_2$ in Third-Generation Ziegler–Natta Catalysts. *J. Appl. Polym. Sci.* **1998**, *69*, 1005–1011.

[13] Taniike, T.; Terano, M. Coadsorption Model for First-Principle Description of Roles of Donors in Heterogeneous Ziegler–Natta Propylene Polymerization. *J. Catal.* **2012**, *293*, 39–50.

[14] Vanka, K.; Singh, G.; Iyer, D.; Gupta, V. K. DFT Study of Lewis Base Interactions with the $MgCl_2$ Surface in the Ziegler–Natta Catalytic System: Expanding the Role of the Donors. *J. Phys. Chem. C* **2010**, *114*, 15771–15781.

[15] Singh, G.; Kaur, S.; Makwana, U.; Patankar, R. B.; Gupta, V. K. Influence of Internal Donors on the Performance and Structure of $MgCl_2$ Supported Titanium Catalysts for Propylene Polymerization. *Macromol. Chem. Phys.* **2009**, *210*, 69–76.

[16] Vittadello, M.; Stallworth, P. E.; Alamgir, F. M.; Suarez, S.; Abbrent, S.; Drain, C. M.; Di Noto, V.; Greenbaum, S. G. Polymeric δ-$MgCl_2$ Nanoribbons. *Inorg. Chim. Acta* **2006**, *359*, 2513–2518.

[17] Di Noto, V.; Fregonese, D.; Marigo, A.; Bresadola, S. High Yield $MgCl_2$-Supported Catalysts for Propene Polymerization: Effects of Ethyl Propionate as Internal Donor on the Activity and Stereospecificity. *Macromol. Chem. Phys.* **1998**, *199*, 633–640.

[18] Fregonese, D.; Glisenti, A.; Mortara, S.; Rizzi, G. A.; Tondello, E.; Bresadola, S. $MgCl_2/TiCl_4/AlEt_3$ Catalytic System for Olefin Polymerisation: A XPS Study. *J. Mol. Catal. A: Chem.* **2002**, *178*, 115–123.

[19] Credendino, R.; Busico, V.; Causà, M.; Barone, V.; Budzelaar, P. H. M.; Zicovich-Wilson, C. Periodic DFT Modeling of Bulk and Surface Properties of $MgCl_2$. *Phys. Chem. Chem. Phys.* **2009**, *11*, 6525–6532.

[20] Busico, V.; Causà, M.; Cipullo, R.; Credendino, R.; Cutillo, F.; Friederichs, N.; Lamanna, R.; Segre, A.; Castelli, V. V. A. Periodic DFT and High-Resolution Magic-Angle-Spinning (HR-MAS) ^1H NMR Investigation of the Active Surfaces of $MgCl_2$-Supported Ziegler–Natta Catalysts. The $MgCl_2$ Matrix. *J. Phys. Chem. C* **2008**, *112*, 1081–1089.

[21] Di Noto, V.; Bresadola, S. New Synthesis of a Highly Active δ-$MgCl_2$ for $MgCl_2/TiCl_4/AlEt_3$ Catalytic Systems. *Macromol. Chem. Phys.* **1996**, *197*, 3827–3835.

[22] Bart, J. C. J. Activation of Magnesium Chloride by Dry Milling. *J. Mater. Sci.* **1993**, *28*, 278–284.

[23] Almeida, L. A.; Marques, M. F. V. Synthesis of a $TiCl_4$ Ziegler–Natta Catalyst Supported on Spherical $MgCl_2$·nEtOH for the Polymerization of Ethylene and Propylene. *Macromol. React. Eng.* **2012**, *6*, 57–64.

[24] Di Noto, V.; Lavina S.; Longo, D.; Vidali, M. A Novel Electrolytic Complex Based on *δ*-$MgCl_2$ and Poly(ethylene glycol) 400. *Electrochim. Acta* **1998**, *43*, 1225–1237.

[25] Jericó, S.; Schuchardt, U.; Joekes, I.; Kaminsky, W.; Noll, A. Chlorinated Organic Polymers as Supports for Ziegler–Natta Catalysts. *J. Mol. Catal. A: Chem.* **1995**, *99*, 167–173.

[26] Nietzel, S.; Joe, D.; Krumpfer, J. W.; Schellenberger, F.; Alsaygh, A. A.; Fink, G.; Klapper, M.; Müllen, K. Organic Nanoparticles as Fragmentable Support for Ziegler–Natta Catalysts. *J. Polym. Sci., Part A: Polym. Chem.* **2015**, *53*, 15–22.

[27] Kaur, S.; Singh, G.; Makwana, U. C.; Gupta, V. K. Immobilization of Titanium Tetrachloride on Mixed Support of $MgCl_2$ · xEB/Poly(methyl acrylate-co-1-octene): Catalyst for Synthesis of Broad MWD Polyethylene. *Catal. Lett.* **2009**, *132*, 87–93.

[28] Kissin, Y. V. Active Centers in Ziegler–Natta Catalysts: Formation Kinetics and Structure. *J. Catal.* **2012**, *292*, 188–200.

[29] Wang, J.; Cheng, R.; He, X.; Liu, Z.; Zhao, N.; Liu, B. Introduction of Chromium Species into the $(SiO_2/MgO/MgCl_2)\cdot TiCl_x$ Ziegler–Natta Catalyst for Better Catalytic Performance. *J. Organomet. Chem.* **2015**, *798*, 299–310.

[30] Tanase, S.; Katayama, K.; Inasawa, S.; Okada, F.; Yamaguchi, Y.; Sadashima, T.; Yabunouchi, N.; Konakazawa, T.; Junke, T.; Ishihara, N. New Synthesis Method Using Magnesium Alkoxides as Carrier Materials for Ziegler–Natta Catalysts with Spherical Morphology. *Macromol. React. Eng.* **2008**, *2*, 233–239.

[31] Smith, G. M.; Tirendi, C. F.; Amata, R. J.; Band, E. I. Alkoxymagnesium Halide Supports for Heterogeneous Ziegler–Natta Polymerization Catalysts. *Inorg. Chem.* **1993**, *32*, 1161–1166.

[32] Mehta, V. C. Preparation of Hydrocarbyloxy-Magnesium Halides. Eur. Pat. Appl. 0294354 A2, 1988.

[33] Smith, G. M.; Amata, R. J.; Tirendi, C. F.; Band, E. I. Halomagnesium Hydrocarbyloxide Composition and Process for Preparation. Eur. Pat. Appl. 0526941 A1, 1993.

[34] Panov, D.; Tuulmets, A.; Nguyen, B. T. Impact of Reaction Products on the Grignard Reaction with Silanes and Ketones. *J. Organomet. Chem.* **2006**, *691*, 4076–4079.

[35] Gulevich, Y.; Camurati, I.; Cristofori, A.; Dall'occo, T.; Morini, G.; Piemontesi, F.; Vitale, G. Magnesium Chloride-Based Adducts and Catalyst Components Obtained Therefrom. PCT Int. Appl. WO 2005/095472 A1, 2005.

[36] Job, R. C. Process for Stable Preparation of Alkoxymagnesium Compounds. U.S. Patent 4,806,696, 1989.

[37] Morini, G.; Cristofori, A.; Gaddi, B.; Liguori, D.; Pater, J. T. M.; Vitale, G. Magnesium Chloroalkolate-Based Catalyst Precursors. PCT Int. Appl. WO 2007/147714 A1, 2007.

[38] Ramjoie, Y. J. E.; Vlaar, M.; Friederichs, N. H.; Sergeev, S. A.; Zakharov, V. A.; Bukatov, G. D.; Taftaf, M.; Aburaqabah, A. Process for Preparing a Catalyst Component for Propylene Polymerization. PCT Int. Appl. WO 2007/134851 A1, 2007.

[39] Turova, N. Ya.; Turevskaya, E. P. Alkoxymagnesium Halides. *J. Organometal. Chem.* **1972**, *42*, 9–17.

[40] Thushara, K. S.; Gnanakumar, E. S.; Mathew, R.; Jha, R. K.; Ajithkumar, T. G.; Rajamohanan, P. R.; Sarma, K.; Padmanabhan, S.; Bhaduri, S.; Gopinath, C. S. Toward an Understanding of the Molecular Level Properties of Ziegler–Natta Catalyst Support with and without the Internal Electron Donor. *J. Phys. Chem. C* **2011**, *115*, 1952–1960.

[41] Brambilla, L.; Zerbi, G.; Piemontesi, F.; Nascetti, S.; Morini, G. Structure of Donor Molecule 9,9-Bis(Methoxymethyl)-Fluorene in Ziegler–Natta Catalyst by Infrared Spectroscopy and Quantum Chemical Calculation. *J. Phys. Chem. C* **2010**, *114*, 11475–11484.

[42] Stukalov, D. V.; Zakharov, V. A.; Potapov, A. G.; Bukatov, G. D. Supported Ziegler–Natta Catalysts for Propylene Polymerization. Study of Surface Species Formed at Interaction of Electron Donors and $TiCl_4$ with Activated $MgCl_2$. *J. Catal.* **2009**, *266*, 39–49.

[43] Potapov, A. G.; Bukatov, G. D.; Zakharov, V. A. DRIFT Study of Internal Donors in Supported Ziegler–Natta Catalysts. *J. Mol. Catal. A: Chem.* **2006**, *246*, 248–254.

[44] Credendino, R.; Pater, J. T. M.; Correa, A.; Morini, G.; Cavallo, L. Thermodynamics of Formation of Uncovered and Dimethyl Ether-Covered $MgCl_2$ Crystallites. Consequences in the Structure of Ziegler–Natta Heterogeneous Catalysts. *J. Phys. Chem. C* **2011**, *115*, 13322–13328.

[45] Correa, A.; Piemontesi, F.; Morini, G.; Cavallo, L. Key Elements in the Structure and Function Relationship of the $MgCl_2/TiCl_4$/Lewis Base Ziegler–Natta Catalytic System. *Macromolecules* **2007**, *40*, 9181–9189.

[46] Turunen, A.; Linnolahti, M.; Karttunen, V. A.; Pakkanen, T. A.; Denifl, P.; Leinonen, T. Microstructure Control of Magnesium Dichloride Crystallites by Electron Donors: The Effect of Methanol. *J. Mol. Catal. A: Chem.* **2011**, *334*, 103–107.

[47] Capone, F.; Rongo, L.; D'Amore, M.; Budzelaar, P. H. M.; Busico, V. Periodic Hybrid DFT Approach (Including Dispersion) to $MgCl_2$-Supported Ziegler–Natta Catalysts. 2. Model Electron Donor Adsorption on $MgCl_2$ Crystal Surfaces. *J. Phys. Chem. C* **2013**, *117*, 24345–24353.

[48] Andoni, A.; Chadwick, J. C.; Niemantsverdriet, H. J. W.; Thüne, P. C. A Flat Model Approach to Ziegler–Natta Catalysts for Propylene Polymerization and a Preparation Method of Well-defined Crystallites of $MgCl_2$-supported Catalysts. *Macromol. Symp.* **2007**, *260*, 140–146.

[49] Andoni, A.; Chadwick, J. C.; Niemantsverdriet, H. J. W.; Thüne, P. C. The Role of Electron Donors on Lateral Surfaces of $MgCl_2$-Supported Ziegler–Natta Catalysts: Observation by AFM and SEM. *J. Catal.* **2008**, *257*, 81–86.

[50] D'Amore, M.; Thushara, K. S.; Piovano, A.; Causà, M.; Bordiga, S.; Groppo, E. Surface Investigation and Morphological Analysis of Structurally Disordered $MgCl_2$ and $MgCl_2/TiCl_4$ Ziegler–Natta Catalysts. *ACS Catal.* **2016**, *6*, 5786–5796.

[51] Cheruvathur, A. V.; Langner, E. H. G.; Niemantsverdriet, H. J. W.; Thüne, P. C. In Situ ATR-FTIR Studies on $MgCl_2$-Diisobutyl Phthalate Interactions in Thin Film Ziegler–Natta Catalysts. *Langmuir* **2012**, *28*, 2643–2651.

[52] Thushara, K. S.; D'Amore, M.; Piovano, A.; Bordiga, S.; Groppo, E. The Influence of Alcohols in Driving the Morphology of $MgCl_2$ Nanocrystals. *ChemCatChem.* doi:10.1002/cctc.201700101.

[53] Stukalov, D. V.; Zakharov, V. A.; Zilberberg, I. L. Adsorption Species of Ethyl Benzoate in $MgCl_2$-Supported Ziegler–Natta Catalysts. A Density Functional Theory Study. *J. Phys. Chem. C* **2010**, *114*, 429–435.

[54] Bazhenov, A.; Linnolahti, M.; Karttunen, A.; Pakkanen, T. A.; Denifl, P.; Leinonen, T. Modeling of Substitutional Defects in Magnesium Dichloride Polymerization Catalyst Support. *J. Phys. Chem. C* **2012**, *116*, 7957–7961.

[55] Bazhenov, A.; Linnolahti, M.; Pakkanen, T. A.; Denifl, P.; Leinonen, T. Modeling the Stabilization of Surface Defects by Donors in Ziegler–Natta Catalyst Support. *J. Phys. Chem. C* **2014**, *118*, 4791–4796.

[56] Kuklin, M.; Bazhenov, A.; Denifl, P.; Leinonen, T.; Linnolahti, M.; Pakkanen, T. A. Stabilization of Magnesium Dichloride Surface Defects by Mono- and Bidentate Donors. *Surf. Sci.* **2015**, *635*, 5–10.

[57] Credendino, R.; Liguori, D.; Fan, Z.; Morini, G.; Cavallo, L. Toward a Unified Model Explaining Heterogeneous Ziegler–Natta Catalysis. *ACS Catal.* **2015**, *5*, 5431–5435.

[58] Chadwick, J. C.; Morini, G.; Balbontin, G.; Camurati, I.; Heere, J. J. R.; Mingozzi, I.; Testoni, F. Effects of Internal and External Donors on the Regio- and Stereoselectivity of Active Species in $MgCl_2$-Supported Catalysts for Propene Polymerization. *Macromol. Chem. Phys.* **2001**, *202*, 1995–2002.

[59] Chadwick, J. C. Advances in Propene Polymerization Using $MgCl_2$-Supported Catalysts. Fundamental Aspects and the Role of Electron Donors. *Macromol. Symp.* **2001**, *173*, 21–35.

[60] D'Amore, M.; Credendino, R.; Budzelaar, P. H. M.; Causá, M.; Busico, V. A Periodic Hybrid DFT Approach (Including Dispersion) to $MgCl_2$-Supported Ziegler–Natta Catalysts – 1: $TiCl_4$ Adsorption on $MgCl_2$ Crystal Surfaces. *J. Catal.* **2012**, *286*, 103–110.

[61] Bazhenov, A.; Denifl, P.; Leinonen, T.; Pakkanen, A.; Linnolahti, M.; Pakkanen, T. A. Modeling Coadsorption of Titanium Tetrachloride and Bidentate Electron Donors on Magnesium Dichloride Support Surfaces. *J. Phys. Chem. C* **2014**, *118*, 27878–27883.

[62] Correa, A.; Credendino, R.; Pater, J. T. M.; Morini, G.; Cavallo, L. Theoretical Investigation of Active Sites at the Corners of $MgCl_2$ Crystallites in Supported Ziegler–Natta Catalysts. *Macromolecules* **2012**, *45*, 3695–3701.

[63] Busico, V.; Cipullo, R.; Monaco, G.; Talarico, G.; Vacatello, M. High-Resolution ^{13}C NMR Configurational Analysis of Polypropylene Made with $MgCl_2$-Supported Ziegler–Natta Catalysts. 1. The "Model" System $MgCl_2/TiCl_4$–2,6-Dimethylpyridine/$Al(C_2H_5)_3$. *Macromolecules* **1999**, *32*, 4173–4182.

[64] Brambilla, L.; Zerbi, G.; Nascetti, S.; Piemontesi, F.; Morini, G. Experimental and Calculated Vibrational Spectra and Structure of Ziegler–Natta Catalyst Precursor: 50/1 Comilled $MgCl_2$-$TiCl_4$. *Macromol. Symp.* **2004**, *213*, 287–301.

[65] Brambilla, L.; Zerbi, G.; Piemontesi, F.; Nascetti, S.; Morini, G. Structure of $MgCl_2$–$TiCl_4$ Complex in Co-Milled Ziegler–Natta Catalyst Precursors with Different $TiCl_4$ Content: Experimental and Theoretical Vibrational Spectra. *J. Mol. Catal. A: Chem.* **2007**, *263*, 103–111.

[66] Cui, N.; Ke, Y.; Li, H.; Zhang, Z.; Guo, C.; Lv, Z.; Hu, Y. Effect of Diether as Internal Donor on $MgCl_2$-Supported Ziegler–Natta Catalyst for Propylene Polymerization. *J. Appl. Polym. Sci.* **2006**, *99*, 1399–1404.

[67] Sacchi, M. C.; Forlini, F.; Tritto, I.; Locatelli, P.; Morini, G.; Noristi, L.; Albizzati, E. Polymerization Stereochemistry with Ziegler–Natta Catalysts Containing Dialkylpropane Diethers: A Tool for Understanding Internal/External Donor Relationships. *Macromolecules* **1996**, *29*, 3341–3345.

[68] Albizzati, E.; Giannini, U.; Morini, G.; Galimberti, M.; Barino, L.; Scordamaglia, R. Recent Advances in Propylene Polymerization with $MgCl_2$ Supported Catalysts. *Macromol. Symp.* **1995**, *89*, 73–89.

[69] Potapov, A. G.; Politanskaya, L. V. The Study of the Adsorption of 1,3-Diethers on the $MgCl_2$ Surface. *J. Mol. Catal. A: Chem.* **2013**, *368–369*, 159–162.

[70] Toto, M.; Morini, G.; Guerra, G.; Corradini, P.; Cavallo, L. Influence of 1,3-Diethers on the Stereospecificity of Propene Polymerization by Supported Ziegler–Natta Catalysts. A Theoretical Investigation on Their Adsorption on (110) and (100) Lateral Cuts of $MgCl_2$ Platelets. *Macromolecules* **2000**, *33*, 1134–1140.

[71] Fregonese, D.; Di Noto, V.; Peloso, A.; Bresadola, S. $MgCl_2$-Supported Catalysts for the Propylene Polymerization: Effects of Triethers as Internal Donors on the Activity and Stereoselectivity. *Macromol. Chem. Phys.* **1999**, *200*, 2122–2126.

[72] Yin, B.; Yi, J.; Chen, S.; Cui, C.; Li, H. A New Method for Dissolving $MgCl_2$ for Preparation of Ziegler–Natta Propylene Polymerization Catalysts. *China Pet. Process. Petrochem. Technol.* **2009**, *3*, 68–70.

[73] Pirinen, S.; Pakkanen, T. T. Polyethers as Potential Electron Donors for Ziegler–Natta Ethylene Polymerization Catalysts. *J. Mol. Catal. A: Chem.* **2015**, *398*, 177–183.

[74] Di Noto, V.; Vittadello, M. Mechanism of Ionic Conductivity in Poly(ethylene glycol 400)/$(MgCl_2)_x$ Polymer Electrolytes: Studies Based on Electrical Spectroscopy. *Solid State Ion.* **2002**, *147*, 309–316.

[75] Yang, Y.; Huo, H. Investigation of Structures of PEO-$MgCl_2$ Based Solid Polymer Electrolytes. *J. Polym. Sci. Part B: Polym. Phys.* **2013**, *51*, 1662–1174.

[76] Auriemma, F.; De Rosa, C. Theoretical Investigation of $(MgCl_2)_x$ Polynuclear Species Formed During Preparation of $MgCl_2$-Supported Ziegler–Natta Catalysts from Solid Solvates. *J. Appl. Cryst.* **2008**, *41*, 68–82.

[77] Malizia, F.; Fait, A.; Cruciani, G. Crystal Structures of Ziegler–Natta Catalyst Supports. *Chem. – Eur. J.* **2011**, *17*, 13892–13897.

[78] Sozzani, P.; Bracco, S.; Comotti, A.; Simonutti, R.; Camurati, I. Stoichiometric Compounds of Magnesium Dichloride with Ethanol for the Supported Ziegler–Natta Catalysis: First Recognition and Multidimensional MAS NMR Study. *J. Am. Chem. Soc.* **2003**, *125*, 12881–12893.

[79] Valle, G. The Crystal Structure of $MgCl_2 \cdot 6C_2H_5OH$. *Inorg. Chim. Acta* **1989**, *156*, 157–158.

[80] Tewell, C. R.; Malizia, F.; Ager, J. W., III; Somorjai, G. A. An Ultraviolet–Raman Spectroscopic Investigation of Magnesium Chloride–Ethanol Solids with 0.47 to 6 Molar Ratio of C_2H_5OH to $MgCl_2$. *J. Phys. Chem. B* **2002**, *106*, 2946–2949.

[81] Dil, E. J.; Pourmahdian, S.; Vatankhah, M.; Taromi, F. A. Effect of Dealcoholation of Support in $MgCl_2$-supported Ziegler–Natta Catalysts on Catalyst Activity and Propylene Powder Morphology. *Polym. Bull.* **2010**, *64*, 445–457.

[82] D'Anna, V.; Norsic, S.; Gajan, D.; Sanders, K.; Pell, A. J.; Lesage, A.; Monteil, V.; Copéret, C.; Pintacuda, G.; Sautet, P. Structural Characterization of the EtOH–$TiCl_4$–$MgCl_2$ Ziegler–Natta Precatalyst. *J. Phys. Chem. C* **2016**, *120*, 18075–18087.

[83] Thushara, K. S.; Mathew, R.; Ajithkumar, T. G.; Rajamohanan, P. R.; Bhaduri, S.; Gopinath C. S. $MgCl_2 \cdot 4(CH_3)_2CHOH$: A New Molecular Adduct and Super Active Polymerization Catalyst Support. *J. Phys. Chem. C* **2009**, *113*, 8556–8559.

[84] Gnanakumar, E. S.; Thushara, K. S.; Gowda, R. R.; Raman, S. K.; Ajithkumar, T. G.; Rajamohanan, P. R.; Chakraborty, D.; Gopinath, C. S. $MgCl_2 \cdot 6C_6H_{11}OH$: A High Mileage Porous Support for Ziegler–Natta Catalyst. *J. Phys. Chem. C* **2012**, *116*, 24115–24122.

[85] Gnanakumar, E. S.; Gowda, R. R.; Kunjir, S.; Ajithkumar, T. G.; Rajamohanan, P. R.; Chakraborty, D.; Gopinath, C. S. $MgCl_2 \cdot 6CH_3OH$: A Simple Molecular Adduct and Its Influence As a Porous Support for Olefin Polymerization. *ACS Catal.* **2013**, *3*, 303–311.

[86] Di Noto, V.; Bresadola, S.; Zanetti, R.; Viviani, M.; Bandoli, G. Crystal Structure of a Magnesium Chloride-Benzyl Alcohol Adduct. *Z. Kristallogr.* **1993**, *204*, 263–270.

[87] Thushara, K. S.; Gnanakumar, E. S.; Mathew, R.; Ajithkumar, T. G.; Rajamohanan, P. R.; Bhaduri, S.; Gopinath C. S. $MgCl_2 \cdot 4((CH_3)_2CHCH_2OH)$: A New Molecular Adduct for the Preparation of $TiCl_x/MgCl_2$ Catalyst for Olefin Polymerization. *Dalton Trans.* **2012**, *41*, 11311–11318.

[88] Sobota, P. Metal-Assembled Compounds: Precursors of Polymerization Catalysts and New Materials. *Coord. Chem. Rev.* **2004**, *248*, 1047–1060.

[89] Sobota, P. Ziegler–Natta Catalyst Intermediates. *Chem. – Eur. J.* **2003**, *9*, 4854–4860.

[90] Pirinen, S.; Koshevoy, I. O.; Denifl, P.; Pakkanen, T. T. A Single-Crystal Model for $MgCl_2$-Electron Donor Support Materials: $[Mg_3Cl_5(THF)_4Bu]_2$ (Bu = n-Butyl). *Organometallics* **2013**, *32*, 4208–4213.

[91] Rönkkö, H.-L.; Knuuttila, H.; Linnolahti, M.; Haukka, M.; Pakkanen T. T.; Denifl, P.; Leinonen, T. Complex Formation and Characterization of $MgCl_2$/2-(2-Ethylhexyloxy)Ethanol Adduct. *Inorg. Chim. Acta* **2011**, *371*, 124–129.

[92] Rönkkö, H.-L.; Knuuttila, H.; Haukka, M.; Pakkanen T. T. ^1H NMR and X-ray Studies on Hydrogen Bonding in Alkyloxy Ethanols and Their $MgCl_2$ Adducts. *Inorg. Chim. Acta* **2011**, *376*, 687–693.

[93] Halut-Desportes, S.; Bois, C. Structure de Chlorure de Magnésium-Pyridine. *Acta Crystallogr., Sect. B: Struct. Crystallogr. Cryst. Chem.* **1979**, *B35*, 2205–2207.

[94] Di Noto, V.; Zanetti, R.; Bresadola, S.; Margio, A.; Marega, C.; Valle, G. Synthesis and Crystal Structure of the $MgCl_2(CH_3COOC_2H_5)_2 \cdot ½(CH_3COOC_2H_5)$ Adduct. *Inorg. Chim. Acta* **1991**, *190*, 279–283.

[95] Di Noto, V.; Bresadola, S.; Zanetti, R.; Viviani, M.; Valle, G.; Bandoli, G. Crystal Structure of a Magnesium Chloride-Ethylformate adduct. *Z. Kristallogr.* **1992**, *201*, 161–170.

[96] Di Noto, V.; Bandoli, G.; Dolmella, A.; Zarli, B.; Viviani, M.; Vidali, M. Crystal Structure of Two Cocrystallized Complexes Obtained from the Reaction of Magnesium Chloride with 2, 4-Pentanedione. *J. Chem. Crystallogr.* **1995**, *25*, 375–378.

[97] Sarma, R.; Ramirez, F.; McKeever, B.; Fen Chaw, Y.; Marecek, J. F.; Nierman, D.; McCaffrey, T. M. Crystal and Molecular Structure of Magnesium Bromide-Tetrahydrofuran Complexes: $MgBr_2(C_4H_8O)_2$, Orthorhombic, and $MgBr_2(C_4H_8O)_4(H_2O)_2$, Triclinic. *J. Am. Chem. Soc.* **1977**, *99*, 5289–5295.

[98] Pércuad, M.-C.; Le Bihan, M.-T. Structure Atomique de $MgBr_2.4C_4H_8O$. *Acta Crystallogr., Sect. B: Struct. Crystallogr. Cryst. Chem.* **1968**, *24*, 1502–1505.

[99] Schibilla, H.; Le Bihan, M.-T. Atomic Structure of $MgBr_2.2Et_2O$. *Acta Crystallogr.* **1967**, *23*, 332–333.

[100] Neumüller, B.; Stieglitz, G.; Dehnicke, K. Die Kristallstruktur von $MgCl_2$(1,2-Dimethoxyethan)$_2$. *Z. Naturforsch., B: J. Chem. Sci.* **1993**, *48*, 1151–1153.

[101] Di Noto, V.; Cecchin, G.; Zanetti, R.; Viviani, M. Magnesium Chloride-Supported Catalysts for Ziegler–Natta Propene Polymerization: Ethyl Formate as Internal Base. *Macromol. Chem. Phys.* **1994**, *195*, 3395–3409

[102] Pirinen, S.; Jayaratne, K.; Denifl, P.; Pakkanen, T. T. Ziegler–Natta Catalysts Supported on Crystalline and Amorphous $MgCl_2$/THF Complexes. *J. Mol. Catal. A: Chem.* **2014**, *395*, 434–439.

[103] Groppo, E.; Seenivasan, K.; Barzan, C. The potential of Spectroscopic Methods Applied to Heterogeneous Catalysts for Olefin Polymerization. *Catal. Sci. Technol.* **2013**, *3*, 858–878.

[104] Gahleitner, M.; Severn, J. R. In *Tailor-Made Polymers: Via Immobilization of Alpha-Olefin Polymerization Catalysts*; Severn, J. R., Chadwick, J. C., Eds.; WILEY-VCH: Weinheim, 2008; pp. 2–5.

[105] Peacock, A. J. *Handbook of Polyethylene*; Marcel Dekker: USA, 2000; pp. 1–55.

[106] Taniike, T.; Chammingkwan, P.; Terano, M. Structure–Performance Relationship in Ziegler–Natta Olefin Polymerization with Novel Core–Shell MgO/$MgCl_2$/$TiCl_4$ Catalysts. *Catal. Commun.* **2012**, *27*, 13–16.

[107] Taniike, T.; Funako, T.; Terano, M. Multilateral Characterization for Industrial Ziegler–Natta Catalysts Toward Elucidation of Structure-Performance Relationship. *J. Catal.* **2014**, *311*, 33–40.

[108] Kissin, Y. V. Main Kinetic Features of Ethylene Polymerization Reactions with Heterogeneous Ziegler–Natta Catalysts in the Light of a Multicenter Reaction Mechanism. *J. Polym. Sci., Part A: Polym. Chem.* **2001**, *39*, 1681–1695.

[109] Kissin, Y. V. Multicenter Nature of Titanium-Based Ziegler–Natta Catalysts: Comparison of Ethylene and Propylene Polymerization Reactions. *J. Polym. Sci., Part A: Polym. Chem.* **2003**, *41*, 1745–1758.

[110] Parvez, M. A.; Rahaman, M.; Suleiman, M. A.; Soares, J. B. P.; Hussein, I. A. Correlation of Polymerization Conditions with Thermal and Mechanical Properties of Polyethylenes Made with Ziegler–Natta Catalysts. *Int. J. Polym. Sci.* **2014**, *2014*, 1–10.

[111] Kissin, Y. V.; Mink, R. I. Ethylene Polymerization Reactions with Multicenter Ziegler–Natta Catalysts–Manipulation of Active Center Distribution. *J. Polym. Sci., Part A: Polym. Chem.* **2010**, *48*, 4219–4229.

[112] Kissin, Y. V.; Zhou, Q.; Li, H.; Zhang, L. Active Centers in Propylene Polymerization Catalysts of the Fourth Generation. *J. Catal.* **2015**, *332*, 156–163.

[113] Kissin, Y. V.; Mink, R. I.; Nowlin, T. E.; Brandolini, A. J. Kinetics and Mechanism of Ethylene Homopolymerization and Copolymerization Reactions with Heterogeneous Ti-Based Ziegler–Natta Catalysts. *Top. Catal.* **1999**, *7*, 69–88.

[114] Taniike, T.; Nguyen, B. T.; Takahashi, S.; Vu, T. Q.; Ikeya, M.; Terano, M. Kinetic Elucidation of Comonomer-Induced Chemical and Physical Activation in Heterogeneous

Ziegler–Natta Propylene Polymerization. *J. Polym. Sci., Part A: Polym. Chem.* **2011**, *49*, 4005–4012.

[115] Arlman, E. J.; Cossee, P. Ziegler–Natta catalysis III. Stereospecific Polymerization of Propene with the Catalyst System $TiCl_3$-$AlEt_3$. *J. Catal.* **1964**, *3*, 99–104.

[116] Iiskola, E.; Koskinen, J. Procedure for Manufacturing Catalyst Components for Polymerizing Olefins. PCT Int. Appl. WO 87/07620, 1987.

[117] Koskinen, J.; Roff, T. Method for the Preparation of a Particulate Carrier for a Polymerization Catalyst. PCT Int. Appl. WO 93/11166, 1993.

[118] Koskinen, J.; Louhelainen, J. Method for Preparing Solid Carrier Particles of Equal Size for Polymerization Catalyst Using Rotating Atomizing Means. PCT Int. Appl. WO 92/21705, 1992.

[119] Vogel, A. I. *A Text-Book of Quantitative Inorganic Analysis Including Elementary Instrumental Analysis*; Longman: London, 1961; pp. 788–790.

[120] Frisch, M. J.; Trucks, G. W.; Schlegel, H. B.; Scuseria, G. E.; Robb, M. A.; Cheeseman, J. R.; Scalmani, G.; Barone, V.; Mennucci, B.; Petersson, G. A., et al. *Gaussian 09*, Revision A.02; Gaussian, Inc.: Wallingford, CT, 2010.

[121] Zhao, Y.; Truhlar, D. G. The M06 Suite of Density Functionals for Main Group Thermochemistry, Thermochemical Kinetics, Noncovalent Interactions, Excited States, and Transition Elements: Two New Functionals and Systematic Testing of Four M06-Class Functionals and 12 Other Functionals. *Theor. Chem. Acc.* **2008**, *120*, 215–241.

[122] Ehm, C.; Antinucci, G.; Budzelaar, P. H. M.; Busico, V. Catalyst Activation and the Dimerization Energy of Alkylaluminium Compounds. *J. Organomet. Chem.* **2014**, *772–773*, 161–171.

[123] Schaefer, A.; Huber, C.; Ahlrichs, R. Fully Optimized Contracted Gaussian Basis Sets of Triple Zeta Valence Quality for Atoms Li to Kr. *J. Chem. Phys.* **1994**, *100*, 5829–5835.

[124] Burwell, R. L., Jr. The Cleavage of Ethers. *Chem. Rev.* **1954**, *54*, 615–685.

[125] Hill, C. M.; Haynes, L.; Simmons, D. E.; Hill, M. E. Grignard Reagents and Unsaturated Ethers. II. Reaction of Grignard Reagents with β,γ-Unsaturated Ethers. *J. Am. Chem. Soc.* **1953**, *75*, 5408–5409.

[126] Hill, C. M.; Haynes, L.; Simmons, D. E.; Hill, M. E. Grignard Reagents and Unsaturated Ethers. VI. The Cleavage of Diallyl Ethers by Aliphatic and Aromatic Grignard Reagents. *J. Am. Chem. Soc.* **1958**, *80*, 3623–3625.

[127] Kharasch, M. S.; Huang, R. L. Factors Influencing the Course and Mechanism of Grignard Reactions. XX. The Cleavage of Ethers by Grignard Reagents in the Presence of Cobaltous Halides. *J. Org. Chem.* **1952**, *17*, 669–677.

[128] Kharasch, M. S.; Stampa, G.; Nudenberg, W. Factors Influencing the Course and Mechanism of Grignard Reactions. XXI. The Reaction of Haloalkyl Phenyl Ethers with Grignard Reagents in the Presence of Cobaltous Halides. *J. Org. Chem.* **1953**, *18*, 575–581.

[129] Kharasch, M. S.; Hancock, J. W.; Nudenberg, W.; Tawney, P. O. Factors Influencing the Course and Mechanism of Grignard reactions. XXII. The Reaction of Grignard Reagents with Alkyl Halides and Ketones in the Presence of Manganous Salts. *J. Org. Chem.* **1956**, *21*, 322–327.

[130] Kharasch, M. S.; Biritz, L.; Nudenberg, W.; Bhattacharya, A.; Yang, N. C. Factors Influencing the Course and Mechanism of Grignard Reactions. XXIII. The Reactions of Propylene Oxide and Related Compounds with Grignard Reagents. *J. Am. Chem. Soc.* **1961**, *83*, 3229–3232.

[131] Kharasch, M. S.; Weiner, M.; Nudenberg, W.; Bhattacharya, A.; Wang, T.; Yang, N. C. Factors Influencing the Course and Mechanism of Grignard reactions. XXIV. Reactions of 1, 3-Disubstituted Compounds, 1,2-Hhydrogen Atom Shift. *J. Am. Chem. Soc.* **1961**, *83*, 3232–3234.

[132] Ohkubo, M.; Mochizuki, S.; Sano, T.; Kawaguchi, Y.; Okamoto, S. Selective Cleavage of Allyl and Propargyl Ethers to Alcohols Catalyzed by Ti(O-*i*-Pr)$_4$/MX$_n$/Mg. *Org. Lett.* **2007**, *9*, 773–776.

[133] Luhtanen, T. N. P.; Linnolahti, M.; Laine, A.; Pakkanen, T. A. Structural Characteristics of Small Magnesium Dichloride Clusters: A Systematic Theoretical Study. *J. Phys. Chem. B* **2004**, *108*, 3989–3995.

[134] Miller, G. J. In *Encyclopedia of Inorganic Chemistry*; King, R. B., Ed.; Wiley: Chichester, 1994; Vol. 3, pp. 1350–1351.

[135] Deng, X.; Yin, Z.; Zhou, Z.; Wang, Y.; Zhang, F.; Hu, Q.; Yang, Y.; Lu, J.; Wu, Y.; Sheng, W.; Zeng Y. Carboxymethyl Dextran-Stabilized Polyethylenimine-Poly(epsiloncaprolactone) Nanoparticles-Mediated Modulation of MicroRNA-34a Expression via Small-Molecule Modulator for Hepatocellular Carcinoma Therapy. *ACS Appl. Mater. Interfaces* **2016**, *8*, 17068–17079.

[136] von Harpe, A.; Petersen, H.; Li, Y.; Kissel, T. Characterization of Commercially Available and Synthesized Polyethylenimines for Gene Delivery. *J. Controlled Release* **2000**, *69*, 309–322.

[137] Leinonen, T.; Denifl, P.; Pöhler, H. Process for Preparing an Olefin Polymerization Catalyst Component with Improved High Temperature Activity. PCT Int. Appl. WO 2004/029112, 2004.

111/2012 KONTKANEN Maija-Liisa: Catalyst carrier studies for 1-hexene hydroformulation: cross-linked poly(4-vinylpyridine), nano zinc oxide and one-dimensional ruthenium polymer

112/2012 KORHONEN Tuulia: The wettability properties of nano- and micromodified paint surfaces

113/2012 JOKI-KORPELA Fatima: Functional polyurethane-based films and coatings

114/2012 LAURILA Elina: Non-covalent interactions in Rh, Ru, Os, and Ag complexes

115/2012 MAKSIMAINEN Mirko: Structural studies of *Trichoderma reesei, Aspergillus oryzae* and *Bacillus circulans* sp. *alkalophilus* beta-galactosidases – Novel insights into a structure-function relationship

116/2012 PÖLLÄNEN Maija: Morphological, thermal, mechanical, and tribological studies of polyethylene composites reinforced with micro– and nanofillers

117/2013 LAINE Anniina: Elementary reactions in metallocene/methylaluminoxane catalyzed polyolefin synthesis

118/2013 TIMONEN Juri: Synthesis, characterization and anti-inflammatory effects of substituted coumarin derivatives

119/2013 TAKKUNEN Laura: Three-dimensional roughness analysis for multiscale textured surfaces: Quantitative characterization and simulation of micro- and nanoscale structures

120/2014 STENBERG Henna: Studies of self-organizing layered coatings

121/2014 KEKÄLÄINEN Timo: Characterization of petroleum and bio-oil samples by ultrahigh-resolution Fourier transform ion cyclotron resonance mass spectrometry

122/2014 BAZHENOV Andrey: Towards deeper atomic-level understanding of the structure of magnesium dichloride and its performance as a support in the Ziegler-Natta catalytic system

123/2014 PIRINEN Sami: Studies on $MgCl_2$/ether supports in Ziegler–Natta catalysts for ethylene polymerization

124/2014 KORPELA Tarmo: Friction and wear of micro-structured polymer surfaces

125/2014 HUOVINEN Eero: Fabrication of hierarchically structured polymer surfaces

126/2014 EROLA Markus: Synthesis of colloidal gold and polymer particles and use of the particles in preparation of hierarchical structures with self-assembly

127/2015 KOSKINEN Laura: Structural and computational studies on the coordinative nature of halogen bonding

128/2015 TUIKKA Matti: Crystal engineering studies of barium bisphosphonates, iodine bridged ruthenium complexes, and copper chlorides

129/2015 JIANG Yu: Modification and applications of micro-structured polymer surfaces

130/2015 TABERMAN Helena: Structure and function of carbohydrate-modifying enzymes

131/2015 KUKLIN Mikhail S.: Towards optimization of metalocene olefin polymerization catalysts via structural modifications: a computational approach

132/2015 SALSTELA Janne: Influence of surface structuring on physical and mechanical properties of polymer-cellulose fiber composites and metal-polymer composite joints

133/2015 CHAUDRI Adil Maqsood: Tribological behavior of the polymers used in drug delivery devices

134/2015 HILLI Yulia: The structure-activity relationship of Pd-Ni three-way catalysts for H_2S suppression

135/2016 SUN Linlin: The effects of structural and environmental factors on the swelling behavior of Montmorillonite-Beidellite smectics: a molecular dynamics approach

136/2016 OFORI Albert: Inter- and intramolecular interactions in the stabilization and coordination of palladium and silver complexes: DFT and QTAIM studies

137/2016 LAVIKAINEN Lasse: The structure and surfaces of 2:1 phyllosilicate clay minerals

138/2016 MYLLER Antti T.: The effect of a coupling agent on the formation of area-selective monolayers of iron α-octabutoxy phthalocyanine on a nano-patterned titanium dioxide carrier

139/2016 KIRVESLAHTI Anna: Polymer wettability properties: their modification and influences upon water movement

140/2016 LAITAOJA Mikko: Structure-function studies of zinc proteins